Inhalable poly(lactic-co-glycolic acid) (PLGA) microparticles encapsulating all-*trans*-Retinoic acid (ATRA) as a host-directed, adjunctive treatment for *Mycobacterium tuberculosis* (Mtb) infection.

Gemma O'Connor[a,b], Nitya Krishnan[c], Aidan Fagan-Murphy[a], Joseph Cassidy[d], Seonadh O'Leary[b], Brian D Robertson[c], Joseph Keane[b], Mary P O'Sullivan[b], Sally-Ann Cryan[a].

Affiliations:

[a]Drug Delivery and Advanced Materials Team, School of Pharmacy, Royal College of Surgeons in Ireland, and Tissue Engineering Research Group, Royal College of Surgeons in Ireland, 123 St Stephens Green, Dublin 2 and Trinity Centre for Bioengineering, Trinity College Dublin, Dublin 2, Ireland and Centre for Research in Medical Devices (CURAM), NUI Galway, Ireland.

[b]Department of Clinical Medicine, Trinity Translation Medicine Institute, St. James's Hospital, Trinity College Dublin, the University of Dublin, Dublin 8, Ireland.

[c]MRC Centre for Molecular Microbiology and Infection, Department of Medicine, Imperial College London, London SW7 2AZ, UK.

[d]Pathobiology Section, UCD School of Veterinary Medicine, University College Dublin, Belfield, Dublin 4, Ireland.

gemmaoconnor@rcsi.ie

nitya.krishnan@imperial.ac.uk

aidanfmurphy@rcsi.ie

joseph.cassidy@ucd.ie

OLEARYSE@tcd.ie

b.robertson@imperial.ac.uk

JKeane@STJAMES.IE

Mary.OSullivan@tcd.ie

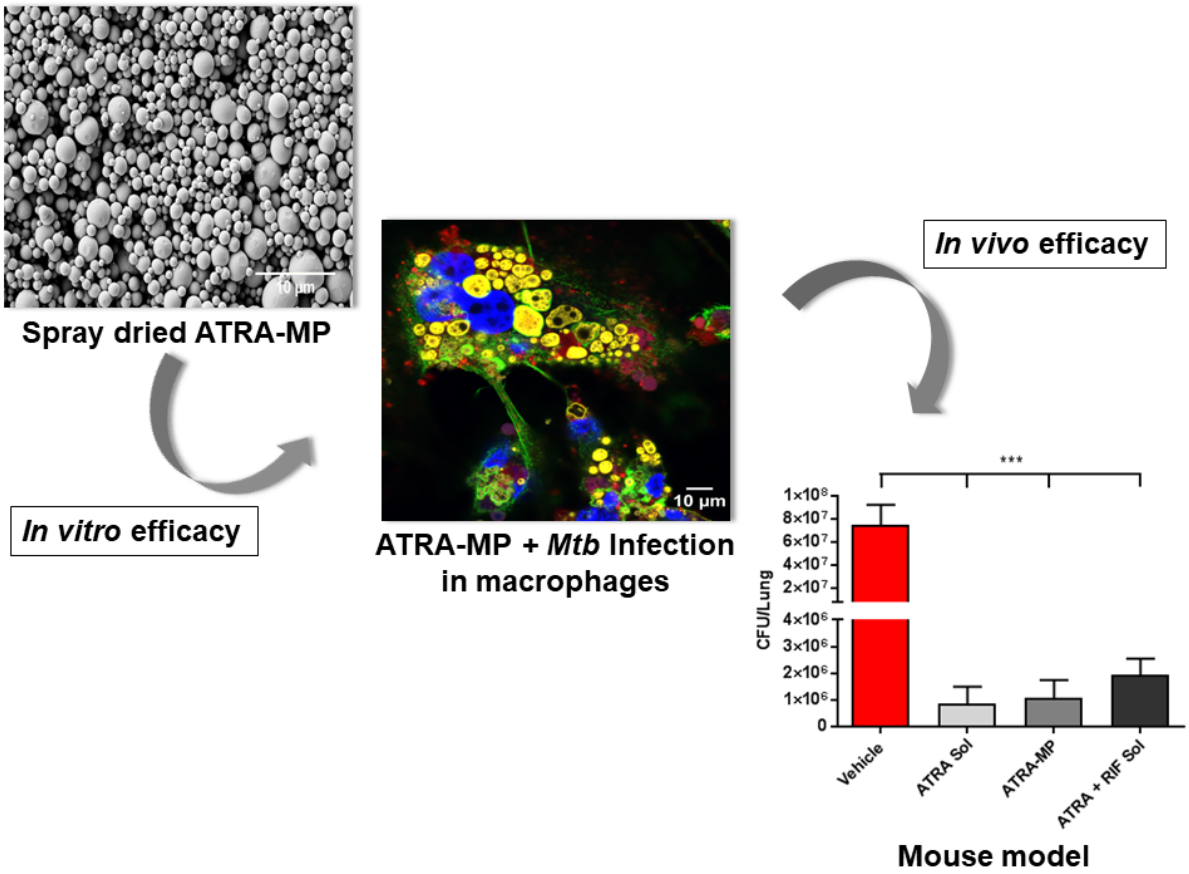
SCryan@rcsi.ie

Corresponding Author: Sally-Ann Cryan SCryan@rcsi.ie

Abstract

Ending the tuberculosis (TB) epidemic by 2030 was recently listed in the United Nations (UN) Sustainable Development Goals alongside HIV/AIDS and malaria as it continues to be a major cause of death worldwide. With a significant proportion of TB cases caused by resistant strains of *Mycobacterium tuberculosis* (Mtb), there is an urgent need to develop new and innovative approaches to treatment. Since 1989, researchers have been assessing the anti-bacterial effects of the active metabolite of vitamin A, all *trans*-Retinoic acid (ATRA) solution, in Mtb models. More recently the antibacterial effect of ATRA has been shown to regulate the immune response to infection via critical gene expression, monocyte activation and the induction of autophagy leading to its application as a host-directed therapy (HDT). Inhalation is an attractive route for targeted treatment of TB, and therefore we have developed ATRA-loaded microparticles (ATRA-MP) within the inhalable size range (2.07 ± 0.5 μm) offering targeted delivery of the encapsulated cargo (70.5 ± 2.3 %) to the site of action within the alveolar macrophage, which was confirmed by confocal microscopy. Efficient cellular delivery of ATRA was followed by a reduction in Mtb growth (H37Ra) in THP-1 derived macrophages evaluated by both the BACT/ALERT® system and enumeration of colony forming units (CFU). The antibacterial effect of ATRA-MP treatment was further assessed in BALB/c mice infected with the virulent strain of Mtb (H37Rv). ATRA-MP treatments significantly decreased the bacterial burden in the lungs alongside a reduction in pulmonary pathology following just three doses administered intratracheally. The immunomodulatory effects of targeted ATRA treatment in the lungs indicate a distinct yet effective mechanism of action amongst the formulations. This is the first study to-date of a controlled release ATRA treatment for TB suitable for inhalation that offers improved targeting of a HDT, retains antibacterial efficacy and improves pulmonary pathology compared to ATRA solution.

Graphical abstract



Keywords

Tuberculosis, all *trans*-Retinoic acid, microparticles, THP-1 cells, mouse model, intratracheal.

1.0 Introduction

Ending the TB epidemic by 2030 was recently listed in the UN Sustainable Development Goals - alongside HIV/AIDS and malaria - since it continues to be major cause of death worldwide, affecting both adults and children (1). With 10.4 million cases of active TB in 2016, an estimated 490 000 of which were multi-drug resistant TB (MDR-TB) (2), there is an obvious need to develop new and innovative approaches to treatment if we are to achieve the UN targets. The pathogen *Mycobacterium tuberculosis* (Mtb) is transmitted via inhalation of infected droplets and its navigation of the airways leads to immune activation and phagocytosis by the alveolar macrophages as well as other phagocytes. Mycobacteria have the ability to block phagolysosomal maturation, avoiding destruction, and can subsequently remain dormant inside the macrophage, which in turn is protected within a granulomatous structure. Conversely, Mtb can continue to multiply in the host cell, resulting in cell rupture, bacterial spread and ultimately lead to active TB disease (3). Thus, macrophages and other components of the immune system, such as cytokines, are critical in the host response to Mtb infection, with any defect caused by conditions such as HIV co-infection (3), diabetes mellitus (4), smoking (5) and alcohol increasing the risk of infection (3). Epidemiological studies have also shown the ill effect of malnutrition and low body mass index on TB susceptibility (6, 7) which is compounded by the fact that the majority (95 %) of TB cases occur in low- to middle-income countries (2).

One approach that has garnered much attention is to augment the immune system in favor of the host in a strategy known as host-direct therapy (HDT) (8-11). In many instances, the HDT's evaluated in the literature are repurposed drugs such as the anti-diabetic drug metformin (12, 13), the cholesterol lowering agent simvastatin (14, 15) and anti-inflammatories including ibuprofen (16) and diclofenac (17). However, endogenous immune activators including interferon-ɣ (IFN-ɣ) (18-20) and interleukin-2 (IL-2) (21, 22) have also been assessed for their potential use in TB treatment resulting in improved clinical outcomes. Another group of possible HDT candidates are vitamins (11) and a recent study by Aibana et al showed that vitamin A deficient adults (≥ 20 years) have a 10-fold increased risk of developing TB and 10-19 year olds had an almost 20-fold increased risk (23). With applications in dermatology and oncology (24), and its use as an "anti-infective" in the early 20th century (25), vitamin A is a multifunctional agent and its active metabolite ATRA has become the focus of a number of TB studies *in vitro* (26-28) and *in vivo* (29-31). The mechanism of action of ATRA in TB is thought to be largely due to its immunomodulatory effects activating monocytes, inducing autophagy and regulating gene expression (27, 28, 32). In addition to the host directed affects, studies have also indicated that ATRA directly reduces bacterial load in culture (33, 34).

There is growing interest in the targeted delivery of anti-tubercular cargoes to the site of pulmonary TB infection in the lungs via inhalation (35-38), including their encapsulation in biocompatible carriers suitable for aerosolisation, so-called therapeutic aerosol bioengineering (TAB) (39). Despite no inhaled treatment for TB reaching the market to-date, studies have been published assessing the potential benefits of a targeted delivery system including polymeric microparticles (40, 41) and lipid based drug delivery systems (42, 43). A phase 1 clinical trial using a dry powder formulation of capreomycin demonstrated the safety of this platform in healthy adult volunteers (44). Vitamin A

treatment is associated with a number of issues including its low aqueous solubility and instability during manufacture and storage due to its sensitivity to light, heat and oxygen (24). In addition, the number of steps required to convert retinol and retinyl esters to ATRA before reaching the target site (45) and toxicities such as photosensitivity could contribute to the lack of efficacy following oral vitamin A supplementation in clinical TB studies to date (46, 47). Previous work by our group demonstrated that poly (Lactide-co-glycolic acid) (PLGA) microparticles (MP) in the size range suitable for inhalation (1 – 5 μm) and alveolar macrophage targeting significantly reduced bacterial viability in Mtb-infected THP-1 derived macrophages when both unloaded (48) and loaded with anti-tubercular cargos (37). Thus, in an effort to bridge the gap between pre-clinical and clinical studies, overcome stability issues and possibly reduce the incidence of resistance resulting from conventional antibiotics, we encapsulated the active metabolite (ATRA) within a targeted, inhalable drug delivery system. To our knowledge, this is the first time ATRA has been encapsulated within PLGA microparticles by spray-drying and used as a treatment within a TB setting *in vitro* and *in vivo*.

The overall aim of this study was to to establish the effect of targeted ATRA treatment on Mtb viability and the host immune responses in both *in vitro* and *in vivo* models of TB. The specific objectives were to develop a controlled release, inhalable treatment using PLGA MPs and assess the effect on: 1) bacterial growth, 2) *in vitro* cell activation, 3) cytokine secretion *in vitro* and gene transcription *in vivo* and 4) the microscopically visible morphological features of the pulmonary lesions.

2.0 Material and methods

2.1 Materials

Poly(D, L-Lactide -co-glycolide) (PLGA) Resomer RG 503 H 50:50 M_w:24,000 – 38,000 Da, rifampicin ≥97 % (HPLC), all-*trans*-Retinoic Acid (ATRA) ≥98 % (HPLC), phosphate buffered saline (PBS), Tween®80, D-Mannitol (≥ 98 %), Dimethyl Sulfoxide Hybri-Max, sterile filtered (DMSO), asparagine, puromycin, bisBenzimide H 33258 and H33342 and HPLC grade solvents were all purchased from Sigma Aldrich Co. LLC, St Louis, MO, USA. Endotoxin free water (BBraun, Ireland). THP-1 cell line and Mtb strain H37Ra were obtained from the American Type Culture Collection (ATCC, Virginia, USA). Mtb strain H37Rv was obtained from Christophe Guilhot, Institut de Pharmacologie et Biologie Structurale, CNRS Toulouse, France. All materials required to prepare Middlebrook 7H9 medium, Middlebrook 7H10 agar and 7H11 agar were purchased from Becton Dickinson (BD, USA). RPMI 1640 Medium and Foetal Bovine Serum (Gibco™). ActinGreen™ 488 ReadyProbes® Reagent, cholera toxin subunit B (Recom) Alexafluor™ 647 conjugate (Invitrogen™) were obtained from Bio-Sciences Ltd., Dublin, Ireland. Modified Auramine O stain and decolourizer were from Scientific Device Laboratory (distributed by Cruinn). Lipopolysaccharide (Alexis). Glycerol, TRIzol, PureLink RNA Mini kit, PureLink DNase and cDNA reverse transcription kit (ThermoFisher Scientific). TaqMan universal master mix and primers (Applied Biosystems).

2.2 The manufacture of MPs by spray-drying

The manufacture of ATRA-loaded PLGA microparticles (ATRA-MPs) was carried out by spray-drying using the Buchi Mini Spray-dyer B-290 with B-295 closed loop system. The closed-loop system allowed optimisation and production of inhalable MPs using the lipid soluble, labile vitamin at the scale required for both *in vitro* and *in vivo* assessment. The feed solution consisted of ATRA: PLGA (1:15) in dichloromethane (DCM) at a polymer concentration of 2 % which was sonicated (Branson 2510 Ultrasonic) for 45 mins immediately prior to use to ensure maximum dissolution. The spray dryer was operated using Nitrogen at 670 L/hr (55 mm), an aspirator rate of 100 %, an inlet temperature of 50˚C and a solution feed rate of 4 ml/min (15 %). The system was flushed with DCM alone before and after running the feed solution to prevent polymer accumulation and all glassware was protected from light throughout the manufacturing process to reduce the risk of ATRA degradation. A depyrogenation protocol was incorporated into the process using endotoxin-free consumables where possible or cleaning equipment with 0.1 M NaOH. Endotoxin levels of the ATRA-MPs were tested post-manufacture using a Pierce™ Limulus Amebocyte Lysate (LAL) Chromogenic Endotoxin Quantitation Kit protocol (Thermo Fisher Scientific, MA, USA). Unloaded PLGA microparticles (UNL-MPs) were utilised as a control formulation in the *in vitro* studies and manufactured by spray-drying using the same parameters listed above for ATRA-MPs.

2.3 The physico-chemical characterisation of MPs

2.3.1 MP size and morphology

The particle size and morphology of ATRA-MPs and UNL-MPs were assessed using scanning electron microscopy (SEM) images. ImageJ software (1.49 v) was employed to verify particle size by first determining the area of a sample of MPs thus allowing calculation of their diameter. SEM was carried out using Zeiss Ultra secondary electron detector at an electron voltage of 5.0 Kv. Prior to analysis each sample was mounted on carbon stubs and coated in gold palladium (10 nm).

2.3.2 ATRA-MP encapsulation efficiency

The encapsulation efficiency of ATRA-MPs was determined by High Performance Liquid Chromatography (HPLC) by firstly dissolving 10 mg of ATRA-MPs in 10 ml of acetone, chosen due to the solubility of both ATRA and PLGA. The sample was then vortexed for 10 mins to release the ATRA from the PLGA before carrying out a 1 in 10 dilution using acetone. In preparation for HPLC the diluted samples were filtered using a 0.45 µm PTFE syringe filter and analysed using the Agilent Technologies 1120 Compact L.C with a Kinetex 5u C18 100 Å (250 x 4.6 mm) (Phenomenex, USA) column and UV detector. The mobile phase consisted of methanol:acetonitrile:water:acetic acid in a ratio of 80:10:10:0.5 which was set to a flow rate of 1 ml/min. The sample injection volume was 10 µl and detection was carried out at 356 nm. The concentration of ATRA in each sample was subsequently determined using the area under the curve and an ATRA standard curve (10.0-0.03 µg/ml) allowing determination of the encapsulation efficiency.

2.3.4 ATRA-MP release study

Owing to their low aqueous solubility, the quantity of ATRA remaining inside the ATRA-MPs was calculated at each time point in order to estimate a release pattern. To do so, 10 mg samples of ATRA-MPs were suspended in light protected tubes containing 5 ml of PBS plus Tween® 80 (0.025 %) at pH 7.4 and pH 5.8 corresponding to each time point. The samples were placed in a shaking water bath at 37˚C. Upon reaching the predetermined time points, the samples were removed from the water bath, centrifuged and the supernatant was separated from the pellet to allow quantification of ATRA remaining encapsulated. Each result was plotted against time to allow estimation of release of ATRA from MPs over a 14-day period.

2.3.5 Aerosolisation properties of ATRA-MP

The aerosol characteristics of the ATRA-MP formulation were evaluated *in vitro* by calculating the percentage of the total dose emitted from a dry powder inhaler using the Dosage Unit Sampling Apparatus (DUSA) (Copley Scientific, UK). Following manufacture of ATRA-MPs by spray-drying, the formulation was suspended in endotoxin-free water (10 mg/ml) and freeze dried (Labconco Freeze

dryer) overnight with mannitol (5 % w/w) to aid flow. The ATRA-MP plus mannitol dry powder (32.7±3.2 mg) was then loaded into size 3 (Gelatin) capsules and, using the Seebri® Breezehaler® (Novartis), assessed with the DUSA operated at an air flow rate of 28.3 L/min for 4.3 sec. Following actuation, the capsules, the inhaler, the DUSA and associated glass fibre filter were all rinsed with PBS-Tween® 80 0.05 % to collect the ATRA-MPs. The quantity of drug in each fraction was calculated by assessment of encapsulated drug in the pellet after centrifugation using the method described earlier for determining encapsulation efficiency.

2.4 *In vitro* assessment of ATRA formulations

2.4.1 Cell culture

THP-1 cells were cultured with complete RPMI (RPMI) consisting of RPMI 1640 medium plus 10% foetal bovine serum (FBS) until required. Prior to analysis, the THP-1 cells were seeded in 12-, 24-, 48- or 96-well Nunc® plates at a density of 1 $X10^5$ cells/ml in 100 nM PMA for 72 to 96 hrs at 37˚C/5% CO_2 to allow differentiation into adherent macrophages. Alongside the cell culture plates, cells were also seeded and differentiated at the same density in Nunc® Lab-Tek II two-well glass chamber slides to allow determination of multiplicity of infection (MOI).

2.4.2 Mycobacterium tuberculosis (Mtb) culture and infection

The avirulent strain Mtb H37Ra (ATCC) was used throughout the series of *in vitro* experiments which were carried out in a biosafety level II safety cabinet and in darkened conditions when ATRA was in-use. Mtb (H37Ra) was propagated in Middlebrook 7H9 medium to log phase at 37˚C/5% CO_2. When required for infection of THP-1 derived macrophages, the Mtb (H37Ra) was firstly centrifuged at 2600 *g* for 10 mins, as previously described (48). The supernatant was discarded, and the remaining pellet was re-suspended in fresh RPMI using a 25 G needle and 5 ml syringe (BD, USA). The suspension was then centrifuged for a further 3 min at 100 *g* to remove any remaining clumps and 5 µl, 25 µl, 50 µl and 250 µl of the resultant suspension was added to the Lab-Tek II chamber slides and incubated at 37˚C/5 % CO_2 for 3 hrs. The MOI was subsequently determined by fixation of the infected THP-1 derived macrophages within the Lab-Tek II chamber slides using 2 % paraformaldehyde. Once fixed, the paraformaldehyde was washed off and stained with Auramine and Hoechst, to visualize acid fast bacteria and cell nuclei. The anti-fade (DAKO) was applied before examining the slides under a 100X oil-immersion objective on a fluorescent microscope (Olympus IX51) using oil. The volume of Mtb suspension required for the desired level of infection was then calculated and added to each well of the NUNC® plates containing THP-1 derived macrophages. The THP-1 derived macrophages were then incubated at 37˚C/5 % CO_2 for 3 hrs to allow the mycobacteria to be phagocytosed. After 3 hrs of incubation the wells were washed with fresh RPMI to remove extracellular mycobacteria followed by addition of treatment as described below.

2.4.3 The effect of ATRA formulations on bacterial growth in macrophages

To assess the antibacterial efficacy of the treatments, THP-1 derived macrophages were infected as above with H37Ra for 3 hrs. After washing to remove extracellular mycobacteria, cells were subsequently incubated with RPMI, ATRA solution (5 µg/ml) and ATRA-MPs (equivalent to 5 µg/ml ATRA) for a total of 192 hr in order to allow an appropriate assessment of its host-directed effects (49). The number of viable mycobacteria 3 hrs post infection were determined to provide a baseline level of infection. The addition of Tween®80 (0.025 %) to RPMI was required to re-suspend the MP formulations therefore RPMI-Tween and UNL-MPs, at the concentration equivalent to that used for ATRA-MP, were used as controls. At 72 hrs and 192 hrs post-treatment, the medium was removed from each well and saved. Meanwhile, 0.1 % Triton-X 100/PBS lysis buffer was added to each well and incubated for 5 mins at room temperature to allow cells to lyse. After 5 mins, the cells were scraped from the wells and added to the corresponding supernatant. Sterile PBS (0.5 ml) was used to wash each well which was also added to the corresponding supernatant. The suspension from each well was then mixed with a 25 G needle and 1 ml syringe to re-suspend the mycobacteria. Change in bacterial growth (%) was assessed using the BacT/ALERT® system (BioMérieux) as previously described (50). Briefly, 0.5 ml of the bacterial suspension from each well was added to the BacT/ALERT® process bottles before being placed in the BacT/ALERT® apparatus. For the CFU assay, dilutions of each suspension were spread, in triplicate, on Middlebrook agar 7H10 plates. The plates were sealed and incubated at 37˚C/5 % CO_2. Between two and three weeks post-treatment the numbers of CFUs visible on each plate were counted allowing viability of mycobacteria to be calculated for each treatment and time point. Rifampicin was not evaluated in the *in vitro* experiments, unlike the *in vivo* studies, due to its sterilising effects in culture (see supplementary Table S.1) and therefore possible masking of the effects of ATRA.

2.4.4 The effect of ATRA formulations on macrophage morphology in vitro

To visualize cell morphology, PMA treated THP-1 cells were seeded directly onto coverslips in a 24-well plate and allowed to differentiate for three days before being incubated with RPMI, ATRA solution (5 µg/ml), ATRA-Rhodamine co-loaded MPs (equivalent to 5 µg/ml ATRA) and UNL-MPs (concentration equivalent to ATRA-Rhodamine-MPs) for 72 hr with and without Mtb infection (H37Ra). At the indicated times, the media was removed, and the cells were washed with PBS and fixed with 2 % paraformaldehyde. After removal of the paraformaldehyde solution, ActinGreen™ 488 (ReadyProbes®), Hoechst (33342 4 µg/ml) and cholera Toxin Subunit B Alexa Fluor® 647 conjugate (1 µg/ml) were applied to stain F-actin, nuclei and cell membranes, respectively. The coverslips were subsequently mounted on a glass slide and analysed by confocal microscopy using the Leica SP8 confocal with 40X oil objective (Leica Microsystems, Wetzlar, Germany).

2.4.5 Cytokine assessment following treatment with ATRA formulations in vitro

A Meso Scale Discovery (MSD®) human pro-inflammatory 7-plex assay was performed using the supernatants from THP-1 derived macrophages treated with RPMI, ATRA solution (5 µg/ml), ATRA-MPs (equivalent to 5 µg/ml ATRA), UNL-MPs (concentration equivalent to ATRA-MPs) and RPMI-Tween® 80 (0.025 %). Evaluation of extracellular cytokine secretion was carried out in the absence or presence of Mtb (H37Ra) infection as per the manufacturer's instructions. Lipopolysaccharide (LPS) from *E.coli* was employed as a positive control. The seven human pro-inflammatory cytokines isolated in this assay were IL-1β, IL-12p70, IFN-ɣ, IL-6, IL-8, IL-10 and TNF-α (only significant data shown).

2.5 *In vivo* assessment of ATRA formulations

2.5.1 Animals

All animal procedures were performed under the licence issued by the UK Home Office (PPL/708653) and in accordance with the Animal Scientific Procedures Act of 1986. Six to eight-week-old female BALB/c mice (Charles River Ltd, UK) were maintained in biosafety containment level 3 facilities according to institutional protocols.

2.5.2 Mycobacterium tuberculosis (H37Rv) infection and growth in vivo following treatment with ATRA formulations

The virulent Mtb strain, H37Rv (Christophe Guilhot, Institut de Pharmacologie et Biologie Structurale, CNRS Toulouse, France) was cultured in Middlebrook 7H9 liquid media supplemented with 0.2% glycerol, 0.05% Tween®80 and 10% oleic acid-albumin-dextrose-catalase (OADC). Mice were infected with 1.84 X 10^3 CFU of H37Rv per mouse via the intranasal route (n=5 mice per group). Two days after infection, 3 mice were humanely culled to determine the number bacteria implanted in the lungs. Following 14 days of infection, mice were treated with ATRA solution (2.5 mg/kg), ATRA-MPs (equivalent to 2.5 mg/kg) and ATRA + rifampicin in solution (2.5 mg/kg + 12mg/kg) as well as the vehicle control (NaCl + Tween®80 0.05 %) via the intra-tracheal route in a final volume of 50 µl, respectively. Each treatment was repeated three times with 48 hrs between each dose. Three days after the final dose (day 21), mice were humanely culled, and lungs aseptically removed. The right lung of each mouse was homogenised in PBS containing 0.05 % Tween-80. The organ homogenates were serially diluted and plated on Middlebrook 7H11 agar plates supplemented with 0.5 % glycerol and 10 % OADC. The number of CFU was enumerated three weeks later. The dose for ATRA treatments was selected following a dose response study (data not shown), keeping in mind the level of toxicity previously reported for this compound (29, 51-57). Rifampicin was added to one treatment group to assess the adjunctive effect of ATRA.

2.5.3 Histological examination of lung following treatment with ATRA formulations

The left lung lobe of each mouse was fixed in 10 % neutral buffered formalin (Sigma-Aldrich, United Kingdom) for histopathological analysis. Approximately 5 µm thick histosections were cut from the paraffin embedded tissues and then stained with the haematoxylin and eosin (H&E) and Ziehl-Neelsen (ZN) stain in each case. The histosections were examined and graded following light microscopy. Lesion grading took into account lesion distribution, size, the constituent cell morphology, evidence of cell necrosis and density/numbers of contained acid-fast organisms. Control and treatment groups were given a semi-quantitative lesion 'score' on a three-point scale (+, mild; ++, moderate, and +++, severe) based on the above histopathological criteria. Between three and five mice were examined per group and photomicrographs of representative lesions taken in each case.

2.5.4 Transcription of pro-inflammatory cytokine genes following treatment with ATRA formulations in vivo

Lung lysates (1 ml) were re-suspended in TRIzol (ThermoFisher Scientific) and total RNA was extracted using the PureLink RNA Mini kit (ThermoFisher Scientific) according to the manufacturer's protocol. Residual DNA from the sample was removed using PureLink DNase (ThermoFisher Scientific). cDNA was generated from 1 µg of RNA using the high-capacity cDNA reverse transcription kit (ThermoFisher Scientific) according to the manufacturer's instructions. Reaction without reverse transcriptase served as the negative control. For real-time PCR, each 20 µl reaction mix contained 10 µl of TaqMan universal master mix (Applied Biosystems), 1 µl of TaqMan primer and probe, 1µl of cDNA and 8 µl of water. Real-time PCR was performed using a SteponePlus PCR machine (Applied Biosystems). Commercially available primers (Applied Biosystems) were used for real-time PCR. Each sample was assayed in duplicates from 5 mice per group. Each gene was normalised to the housekeeping gene, GAPDH and expressed as ΔC_T.

2.6 Statistics

Statistical analysis of results was carried out using GraphPad Prism software, version 7.03. Results were expressed as mean ± standard deviation in tables and figures. A two-way ANOVA was carried out on all toxicity, *in vitro* efficacy and cytokine data followed by a Bonferroni post hoc test. A one-way ANOVA was carried out on all *in vivo* efficacy and transcription data followed by a Tukey multiple comparison test. The *p value* was considered significant when < 0.05.

3.0 Results

3.1 MP physico-chemical characterisation

3.1.1 MP size, morphology and encapsulation efficiency

The size and morphology of ATRA-MPs and UNL-MPs were determined using SEM and ImageJ software resulting in a geometric particle size of 2.07 ± 0.5 µm and 1.91 ± 0.4 µm, respectively, alongside spherical morphology in both groups (Fig. 1 (A-D)). These results are within the requirements for alveolar macrophage uptake as previously determined (58). An encapsulation efficiency of 70.5 ± 2.3 % (47.2 ± 1.5 µg/mg ATRA/MP) was achieved for ATRA-MPs allowing targeting of the cargo to the site of action.

3.1.2 ATRA-MP release study

To estimate release of the lipophilic molecule ATRA in PBS, the quantity of the ATRA remaining encapsulated within ATRA-MPs at each time point was measured. Steadily decreasing quantities of encapsulated ATRA were found over a 14-day period indicating controlled release of the lipophilic cargo (Fig. 1 (E)) as it diffuses through the polymer matrix. Similar release patterns were exhibited at both pH 7.4 and pH 5.8 signifying suitable release both at physiological pH and within the target site, the alveolar macrophage, where the pH varies from 6.2 in the early phagosome to 4.5 in the lysosome (59).

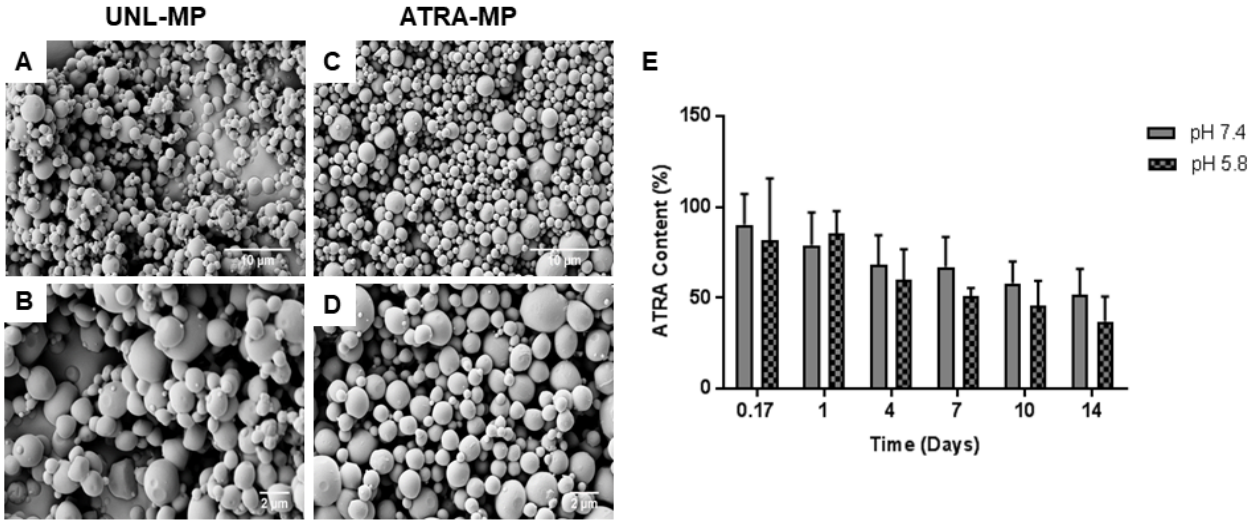


Figure 1: Physico-chemical characterisation of microparticles manufactured by spray drying. Unloaded-MPs (UNL-MPs) and ATRA-loaded MPs (ATRA-MP) display the size and morphology suitable for alveolar deposition. The representative Scanning Electron Microscope (SEM) images were taken using the Zeiss Ultra secondary electron detector at an electron voltage of 5.0Kv and a magnification of (A) 2.53kx and (B) 5.58kx for UNL-MPs and (C) 2.53kx and (D) 5.35kx for ATRA-MPs. (E) The content of ATRA (%) remaining within ATRA-MP suspended in phosphate buffered saline (PBS) + Tween® 80 0.025% at pH 7.4 and 5.8 was measured by high performance liquid chromatography (HPLC). Samples were taken over a 14-day period to allow estimation of release from the drug delivery system, (n=3 ± SD).

3.1.3 Aerosolisation properties of ATRA-MPs

The emitted dose of the ATRA-MP formulated with mannitol from a dry powder inhaler Seebri® Breezehaler® (Novartis) was found to be 53.7 ± 21.5 %. Approximately half of the dose was therefore available for delivery to the lower airways allowing targeted delivery of the cargo, although there was considerable variability amongst samples. Dry powder formulations, such as this, require efficient de-agglomeration on exit from the inhalation device to ensure sufficient flow and movement through the respiratory system. Any influence on the stability of the formulation including moisture or humidity can affect the flow and therefore should be monitored throughout manufacture and storage to improve the reproducibility.

3.2 In vitro assessment of ATRA treatment

3.2.1 The effect of ATRA treatment on bacterial growth in macrophages

Differentiated THP-1 macrophages were infected with Mtb H37Ra at an MOI of 1-10 bacilli per cell for 3 hrs after which the extracellular mycobacteria were washed off, ATRA treatments were added and the cells were incubated for 72 hrs to 192 hrs. The effect of ATRA treatment on Mtb growth was assessed using the BacT/ALERT® liquid culture system measuring time to positivity (TTP) (Fig.2 (A)) and also by enumeration of CFU (CFU/10^5 cells) (Fig.2 (B)) on Middlebrook agar. At 72 hr post-treatment ATRA solution reduced bacterial growth in comparison to untreated controls. At 192 hrs both ATRA solution and ATRA-MP significantly reduced bacterial growth (Fig. 2 (A)), a result which was later verified by CFU enumeration (Fig. 2 (B)). ATRA in solution was significantly better (**$p < 0.01$) at reducing bacterial growth at 192 hrs using the BacT/ALERT® system (Fig. 2 (A)), although no significant difference was found between these treatments in the CFU assay at this timepoint (Fig. 2 (B)). The cytotoxicity of ATRA formulations was also determined by Propidium Iodide (PI) exclusion assay in uninfected and Mtb infected (H37Ra) THP-1 cells *in vitro* 24 hrs, 72 hrs and 192 hrs post-treatment (See supplementary Figure S1). The proportion of PI positive cells following treatment with ATRA solution and ATRA-MPs remained < 25 % under all test conditions and for the control treatments, the MP vehicle (RPMI + Tween® 80 0.025 %) did not significantly induce cell death at any time point.

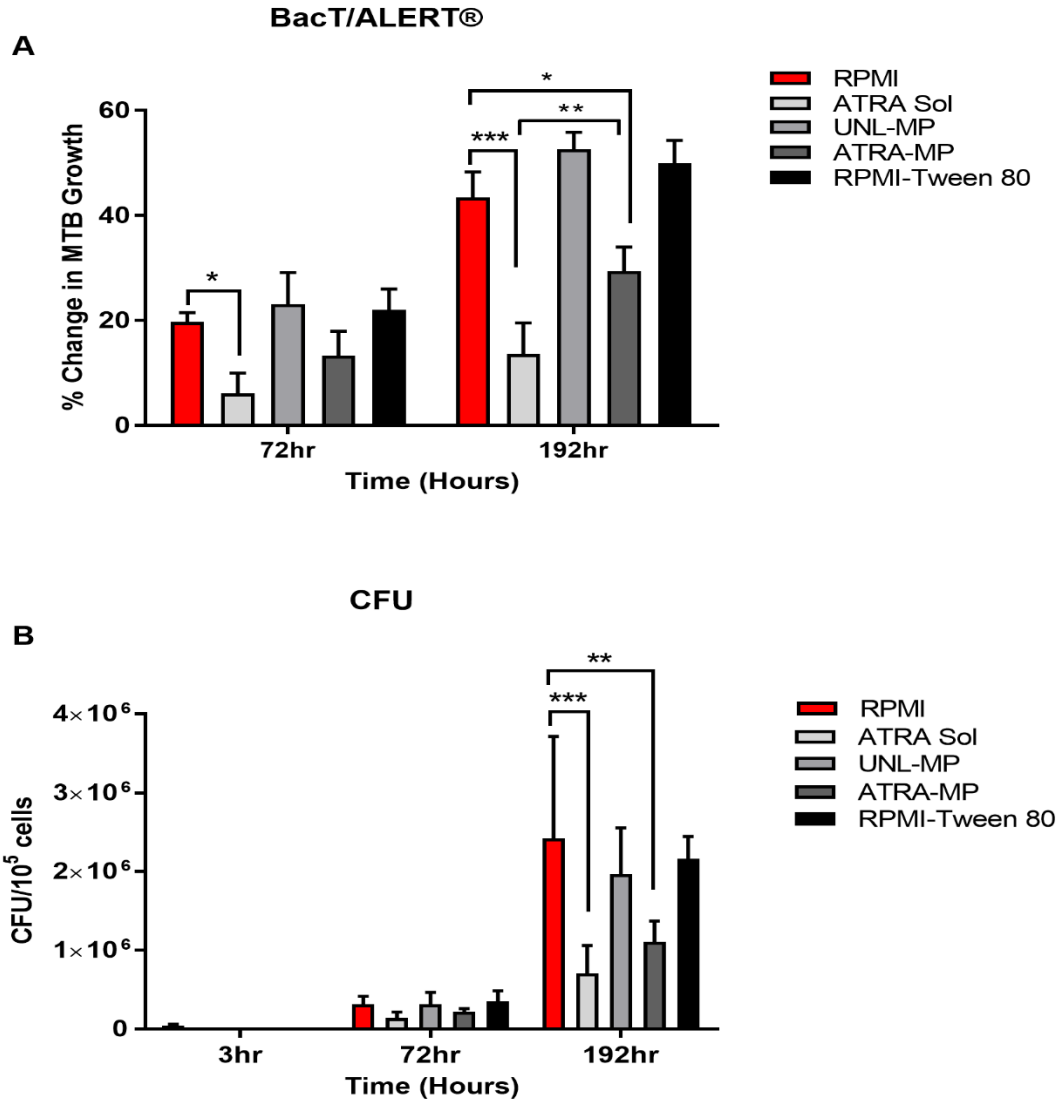


Figure 2: ATRA treatment arrests growth of Mtb (H37Ra) *in vitro*. Baseline infection levels were measured at 3 hrs post-infection of THP-1 derived macrophages with H37Ra which was followed by the addition of treatment. Treatment groups included RPMI, ATRA solution (5 µg/ml), unloaded-MPs (UNL-MP), ATRA-loaded MPs (ATRA-MP) (equivalent to 5 µg/ml ATRA) and RPMI-Tween® 80 0.025%. Efficacy of treatment was assessed at 72 hrs and 192 hrs post-treatment by monitoring (A) the change in bacterial growth (%) using the BacT/Alert® 3D system (BioMérieux), MOI:1-6/cell (n=3) and (B) bacterial viability via enumeration of colony forming units (CFU/ml) on Middlebrook 7H10 agar, MOI: 1-10/cell (n=3) with *$p < 0.05$, **$p < 0.01$ and ***$p < 0.001$.

3.2.2 The effect of ATRA treatment on macrophage morphology in vitro

Treatment of THP-1 derived macrophages with ATRA solution and ATRA-MPs resulted in morphological changes in both the absence (Fig. 3 (A)) and presence (Fig. 3 (B)) of Mtb infection (H37Ra). Treatment with ATRA formulations led to the development of pseudopodia not seen in the RPMI and UNL-MP (equivalent to ATRA-rhodamine-MP concentration) treated groups. The ATRA treated cells became elongated and began to fuse with neighboring cells. This result was confirmed by cell membrane (cholera Toxin B; red) and F-actin (ActinGreen™; green) staining whereby there was no apparent membrane in the cell structure between fused cells. The formation of multi-nucleated cells was also visible using Hoechst (blue) in the ATRA treated, Mtb infected cells (Fig. 3 (B)) with three to four nuclei present in cells. In the case of ATRA-MPs, efficiency in MP uptake (rhodamine; yellow) and, therefore, exposure of cells to the encapsulated ATRA was also established at 72 hrs post-treatment with the presence of many MPs (<10 μm) visible in the cytoplasm of uninfected and infected cells.

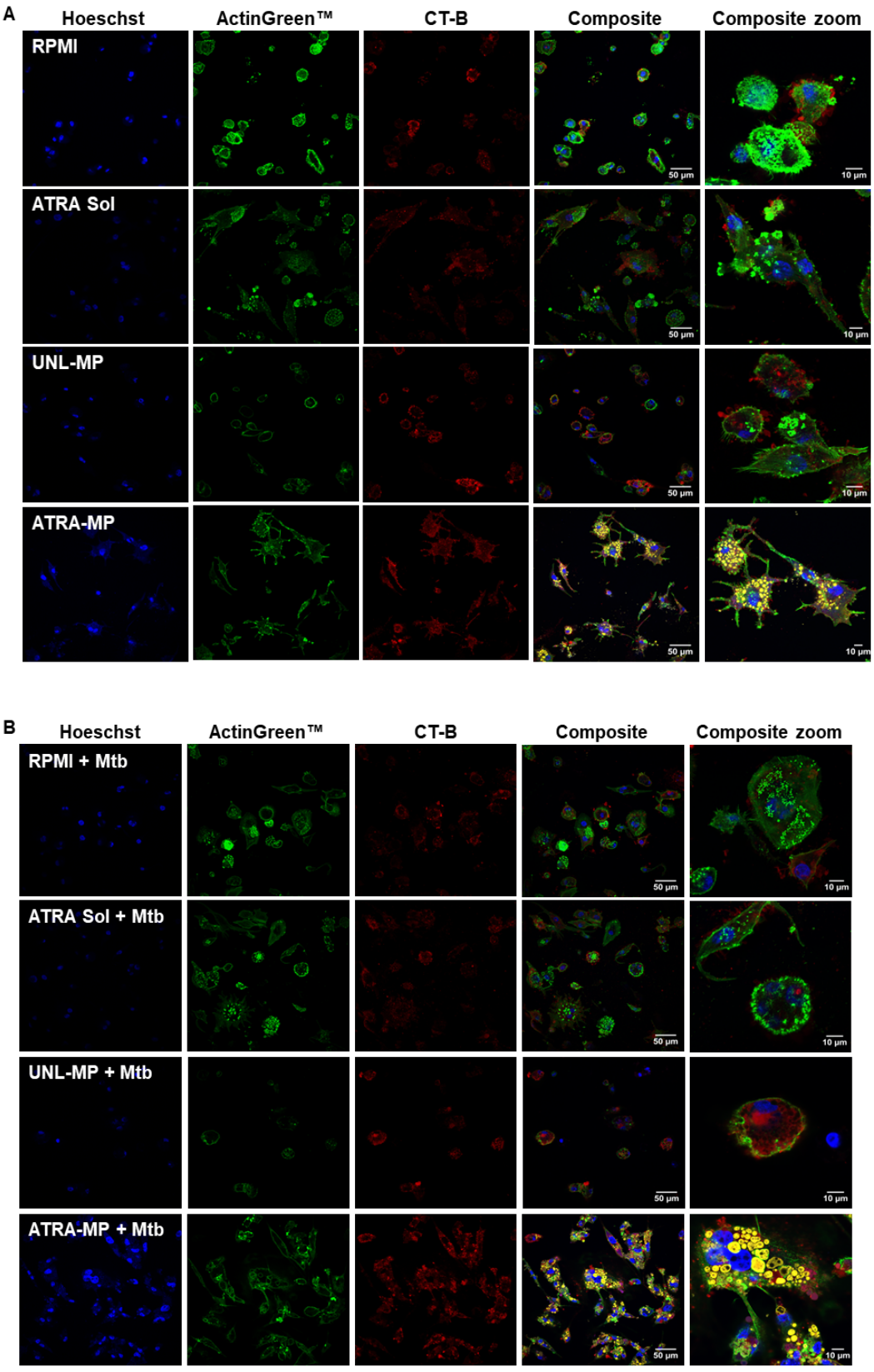
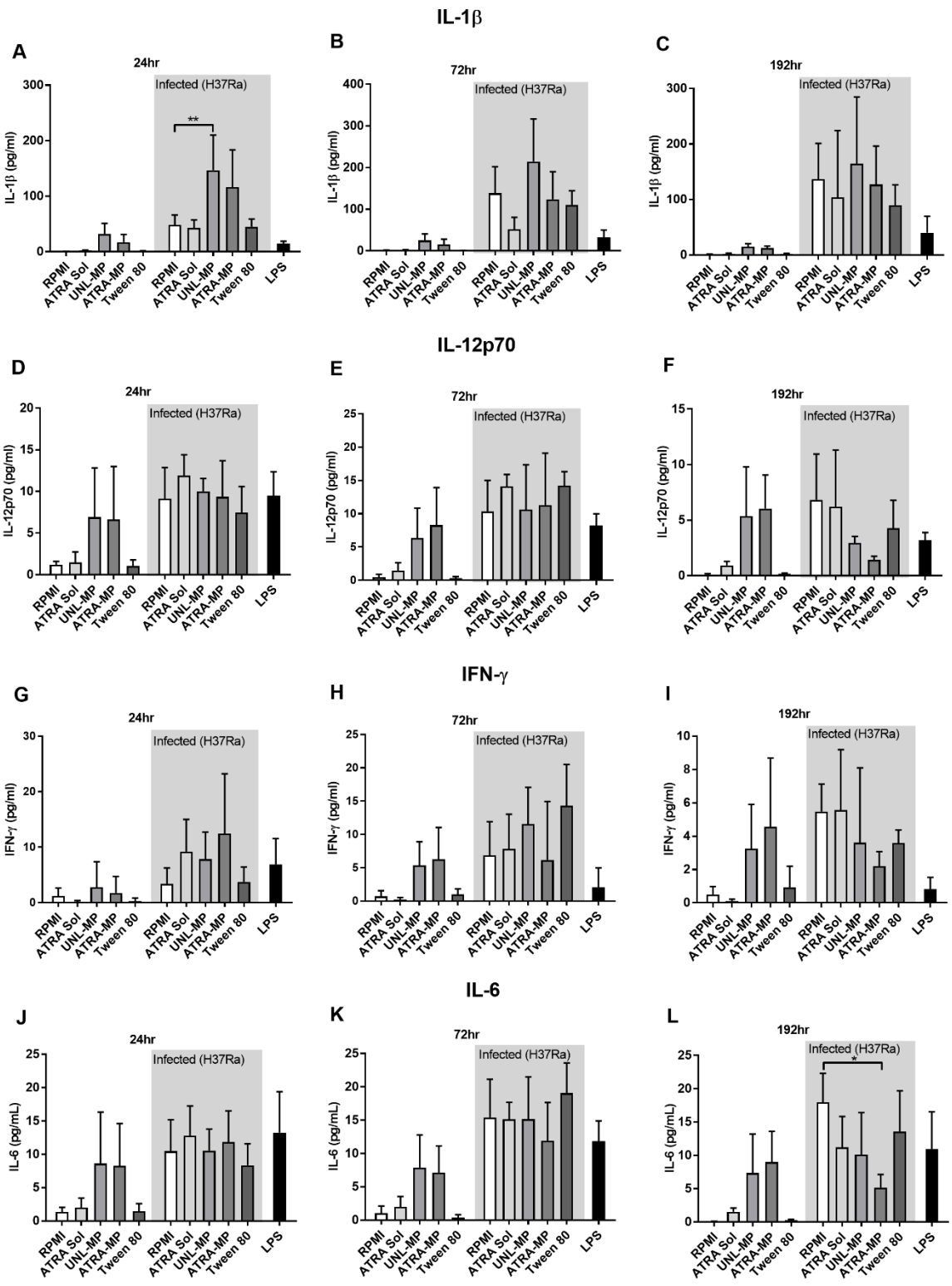


Figure 3: Cell morphology following ATRA treatment for 72 hrs. THP-1 derived macrophages were treated with RPMI, ATRA solution (5 µg/ml), unloaded-MPs (UNL-MP) and ATRA-rhodamine-MPs (ATRA-MP) (equivalent to 5 µg/ml ATRA) in the absence (A) and presence of Mtb infection (B) and viewed 72 hr later using confocal microscopy. Hoechst (blue), ActinGreen™ (green) and cholera Toxin B (red) were added to allow visualisation of the nucleus, cell actin and cell membrane respectively. ATRA-MPs included rhodamine (yellow) to highlight cell uptake.

3.2.3 Cytokine assessment following ATRA treatment in vitro

A panel of pro-inflammatory cytokines including IL-1β, IL-12p70, IFN-ɣ, IL-6, IL-8, IL-10 and TNF-α were measured in the supernatants of THP-1 derived macrophages 24 hrs, 72 hrs and 192 hrs post-treatment with ATRA formulations. At 24 hrs post-treatment, UNL-MPs significantly increased TNF-α in uninfected cells (Fig. 4 (S)) compared to the untreated control (RPMI). There were no significant differences between treatments in infected or uninfected cells at 72 hrs. Infection with H37Ra increased the secretion of cytokines above that of uninfected control cells at all time points examined. Treatment with UNL-MPs significantly increased IL-1β secretion in Mtb-infected cells (Fig. 4 (A) above the level secreted by infected cells alone. Treatment with ATRA-MP also increased IL-1β secretion in Mtb-infected cells although this did not reach statistical significance. Secretion of IL-10 was significantly decreased 196 hrs after infection by treatment with ATRA solution, unloaded MPs and ATRA-MPs (Fig. 4 (R); ***$p < 0.001$). In addition, at 192 hrs post-treatment ATRA-MPs significantly decreased pro-inflammatory IL-6 secretion (Fig. 4 (L)).


IL-1β
A
24hr
Infected (H37Ra)
IL-1β (pg/ml)
**
B
72hr
Infected (H37Ra)
IL-1β (pg/ml)
C
192hr
Infected (H37Ra)
IL-1β (pg/ml)
IL-12p70
D
24hr
Infected (H37Ra)
IL-12p70 (pg/ml)
E
72hr
Infected (H37Ra)
IL-12p70 (pg/ml)
F
192hr
Infected (H37Ra)
IL-12p70 (pg/ml)
IFN-γ
G
24hr
Infected (H37Ra)
IFN-γ (pg/ml)
H
72hr
Infected (H37Ra)
IFN-γ (pg/ml)
I
192hr
Infected (H37Ra)
IFN-γ (pg/ml)
IL-6
J
24hr
Infected (H37Ra)
IL-6 (pg/mL)
K
72hr
Infected (H37Ra)
IL-6 (pg/mL)
L
192hr
Infected (H37Ra)
*
IL-6 (pg/mL)
RPMI
ATRA Sol
UNL-MP
ATRA-MP
Tween 80
LPS

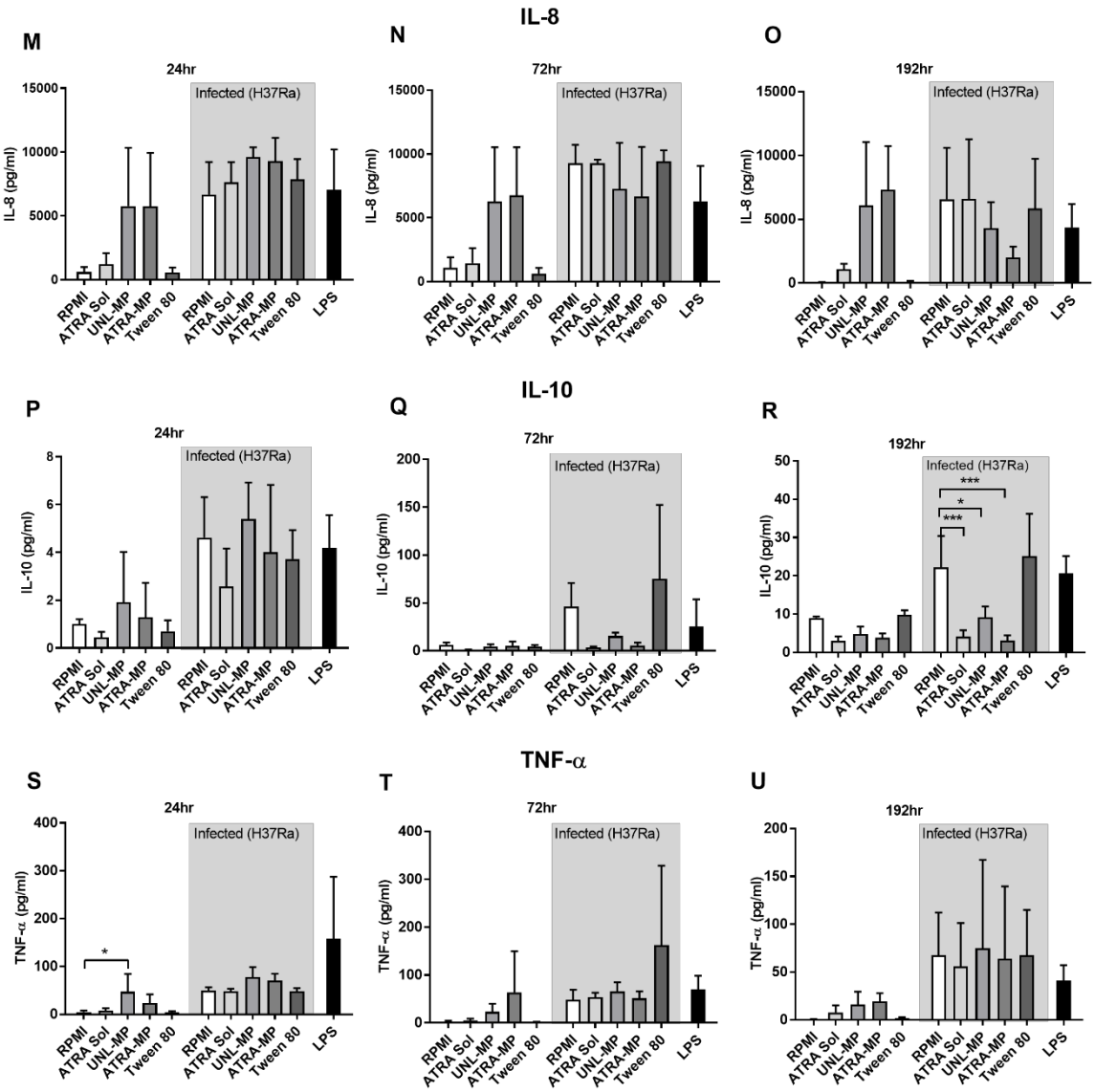


Figure 4: ATRA treatment modulates extracellular cytokine activity in the presence and absence of Mtb infection (H37Ra). The quantity (pg/ml) of cytokine in the supernatant of THP-1 macrophages was measured 24hrs, 72hrs and 192hrs post-treatment with RPMI, ATRA solution (5 µg/ml), unloaded-MPs (UNL-MP), ATRA-loaded MPs (equivalent to 5 µg/ml ATRA) and RPMI-Tween® 80 (0.025 %). (A-C) IL-1β, (D-F) IL-12p70, (G-I) IFN-ɣ (J-L), IL-6, (M-O) IL-8, (P-R) IL-10 and (S-U) TNF-α. Cytokine studies were carried out in the presence and absence of Mtb infection (H37Ra) using a MSD® human pro-inflammatory 7-plex assay and lipopolysaccharide (LPS) as a positive control (n=3), *p < 0.05, **p < 0.01 and ***p < 0.001

3.3 *In vivo assessment of ATRA treatment*

3.3.1 The effect of ATRA treatment on bacterial growth in vivo

In an acute model of Mtb infection BALB/c mice were infected intranasally with H37Rv. Three doses of ATRA in solution, ATRA MPs or ATRA plus rifampicin in solution were administered intratracheally at 48 hr intervals starting on day 14. By day 21 post infection ATRA solution and ATRA-MPs significantly reduced the bacterial load in in the lungs of Mtb infected (H37Rv) BALB/c mice (CFU/lung) to an average of 8.7 x 10^5 CFU/lung and 1.08 x 10^6 CFU/lung, respectively in comparison to the vehicle control of 7.5 x 10^7 CFU/lung (Fig. 5). The addition of rifampicin solution to ATRA solution also resulted in a significant reduction in CFU/lung, comparable to ATRA alone signifying no interaction or weakening of the effect of ATRA in the presence of the antibiotic. There was no significant difference between the treatment groups (Fig. 5). UNL-MPs administered in the same *in vivo* model (BALB/c mice + H37Rv) at a higher concentration (equivalent to 20 mg/kg of ATD cargo) had no effect on bacterial load (see supplementary Figure S.2)

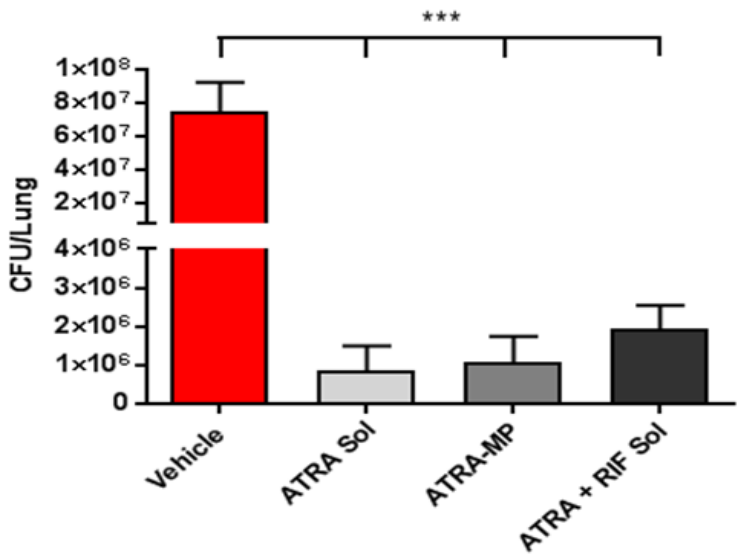


Figure 5: ATRA treatment reduces Mtb (H37Rv) growth *in vivo*. BALB/c mice infected with Mtb (H37Rv) were treated 14 days post-infection with vehicle only (NaCl 0.9% + 0.05% Tween®80), ATRA solution (2.5 mg/kg), ATRA-loaded MPs (ATRA-MP) (equivalent to 2.5mg/kg ATRA) and ATRA plus rifampicin solution (2.5 mg/kg + 12 mg/kg). Three doses of each treatment were administered 48 hrs apart. Bacterial viability was measured by harvesting Mtb from the lung of the animals and plating on Middlebrook 7H11 agar 21 days post-infection, colonies were counted a further 21 days later (n=5).

3.3.2 Histological examination of lung lobes following ATRA treatment

Lungs of infected BALB/C mice treated with ATRA-MP and ATRA solution plus rifampicin showed reduced lesion size and overall pulmonary pathology in comparison to the vehicle control and ATRA solution alone (Fig. 6). The extent of perivascular lymphocytic accumulations did not differ amongst treatment and control groups and the ZN stain indicated no apparent difference in the density of acid-fast bacteria.

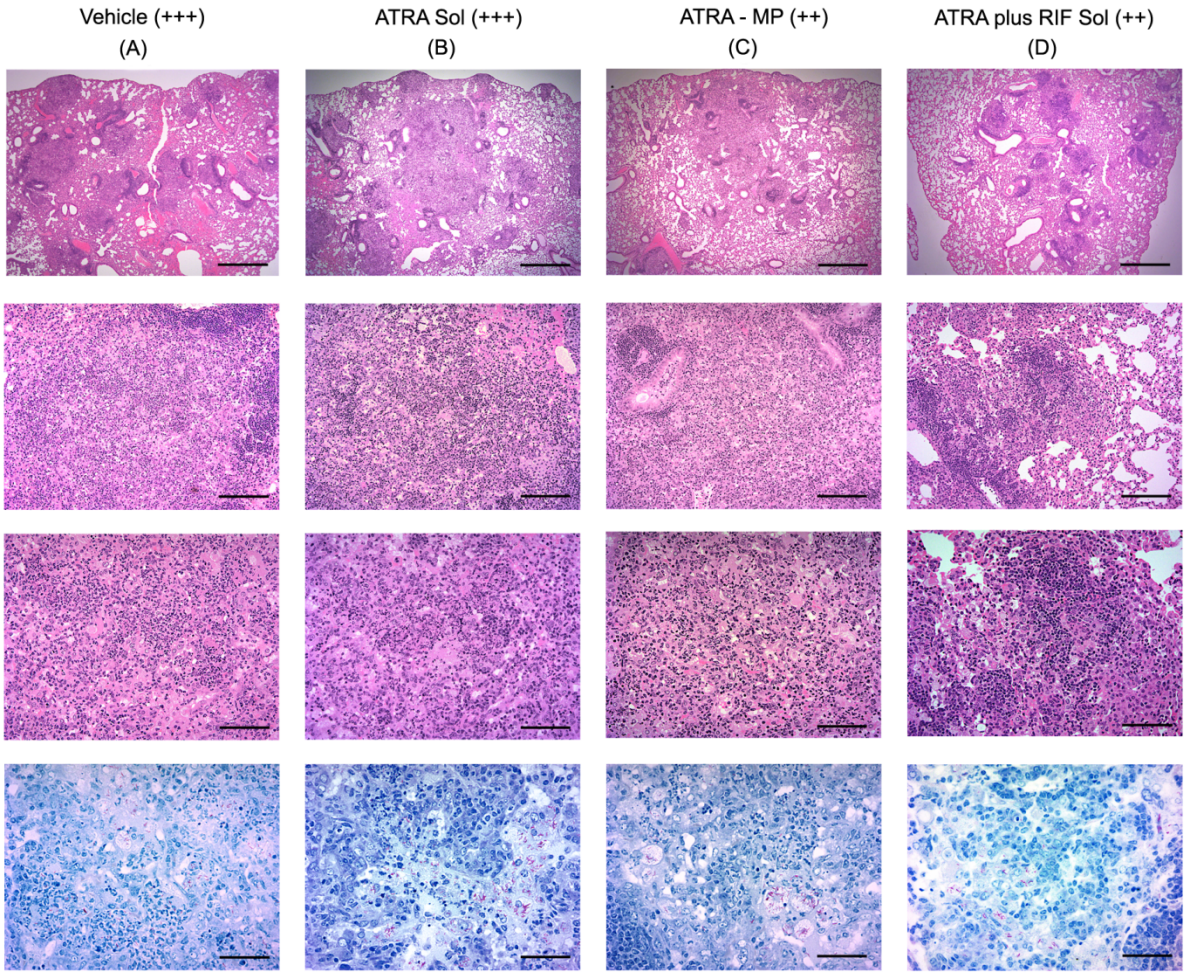


Figure 6: Treatment with encapsulated (ATRA-MP) and adjunctive ATRA solution plus rifampicin result in reduced pulmonary pathology in mice following Mtb (H37Rv) infection. Representative photomicrographs of the left lung from BALB/C mice 21 days post-infection with Mtb (H37Rv) following treatment with vehicle (NaCl+Tween®80 0.05%) (column A), ATRA solution (2.5mg/kg) (column B), ATRA-loaded MPs (equivalent to 2.5mg/kg ATRA) (column C) and ATRA plus rifampicin solution (2.5mg/kg + 12mg/kg) (column D). Lung histosections were stained using the haematoxylin and eosin (x2, x10, x20) and Ziehl–Neelsen (x40ZN) techniques and graded using a semi-quantitative scoring system right (+++, severe, ++, moderate and +, mild). Pulmonary inflammation in the ATRA-MP and ATRA+RIF sol treatment groups (columns C and D) was less extensive than the 'vehicle' (column A) and 'ATRA sol' (column B) treatment groups. The density of acid-fast bacteria visualised was similar in all four treatment groups (bottom micrograph of each column.

3.3.3 Transcription of pro-inflammatory cytokine genes following treatment with ATRA formulations in vivo

Analysis of the effect of ATRA treatment on the transcription of pro-inflammatory cytokine genes in lung homogenates was carried out in parallel with the *in vivo* efficacy testing. Genetic probes were selected to match the pro-inflammatory cytokine panel analysed *in vitro* with the addition of IL-17, inducible nitric oxide synthase (iNOS) and the ATRA response genes CYP27A1 and NPC2 - which regulates lysosomal lipid storage. ATRA treatments resulted in a variable transcription profile from most of the cytokines with the exception of TNF-α whose transcription was significantly increased, compared to vehicle control, by ATRA in solution alone and in combination with rifampicin (Fig. 7 (A)). In addition, iNOS transcription was significantly decreased in ATRA-MP-treated lungs, while ATRA solution alone, or in combination with rifampicin, had no effect compared to the vehicle control (Fig. 7 (B)). CYP27A, NPC2 and all other genes assessed were not significantly altered by encapsulated or nonencapsulated ATRA (see supplementary Figure S.3).

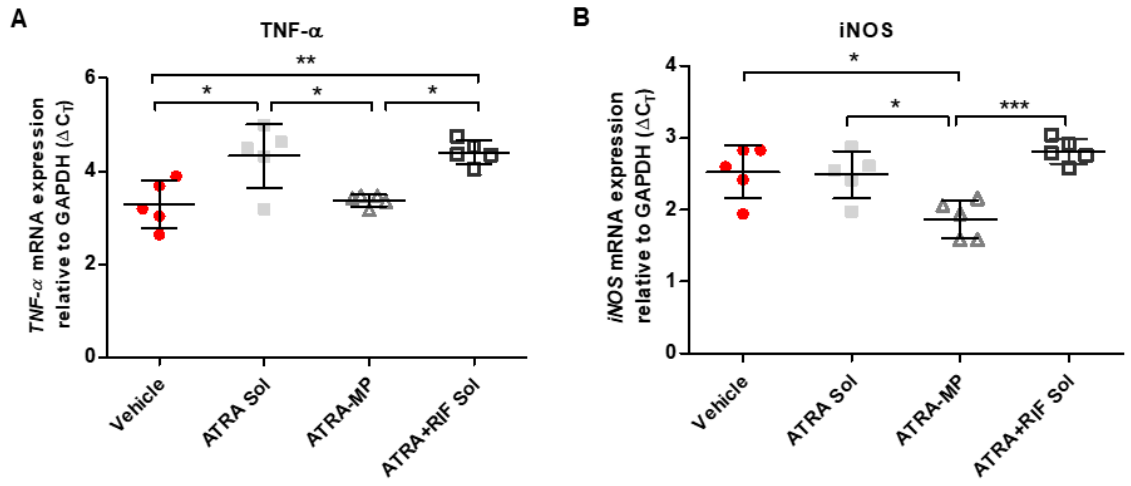


Figure 7: ATRA solution promotes TNF-α transcription in the murine lung while ATRA-MPs reduce the transcription of iNOS. *In vivo* mRNA expression analysis following treatment of Mtb (H37Rv) infected BALB/C mice with vehicle (NaCl+Tween®80 0.05%), ATRA solution (2.5 mg/kg), ATRA-loaded MPs (equivalent to 2.5 mg/kg ATRA) and ATRA plus rifampicin solution (2.5 mg/kg + 12 mg/ml). Real time PCR analysis was carried out on lung homogenates 21 days post-infection and expressed relative to GAPDH (ΔC_T). (A) TNF-α, (B) iNOS (n=5).

4.0 Discussion

A targeted drug delivery platform with the potential to reduce the dosage and/or toxicity burden typically associated with TB treatment and to overcome the emerging issues associated with resistance is currently of enormous scientific and clinical interest. Many studies have focused on the use of PLGA MPs as a biocompatible carrier for antibiotics (35-37, 60, 61) while others have revealed the possible benefit of pulmonary administration of rifampicin for TB, in the form of porous particles, over the oral and intravenous routes (62). With this in mind, we sought to combine the well-defined PLGA microparticulate carrier system with the potential benefits of a HDT to develop a targeted treatment that simultaneously beneficially modulates the immune system via encapsulated cargo. With an overall objective of establishing the effect of targeted ATRA treatment on Mtb viability and the host immune response, we found that an inhalable ATRA-MP formulation targeted ATRA to the macrophages and significantly reduced the bacterial load in pre-clinical models of TB. ATRA-MPs also induced both pro- and anti-inflammatory host responses leading to less severe pulmonary pathology in Mtb (H37Rv) infected mice following treatment. Taken together, the findings support combining MPs and ATRA to create a bioactive formulation.

Suitable aerosol properties, such as particle size and flow, are essential for the successful development of a formulation for inhalation. The ATRA-MP formulations demonstrated suitability for alveolar targeting based on previous studies whereby a diameter of 0.8 – 2.7 μm was determined as optimal (35, 37, 58, 63). Despite lower encapsulation of ATRA within spray-dried MPs when compared to that of traditional antibiotics (40, 63), the encapsulation efficiency of ATRA-MPs (70.5 ± 2.3 %) is in line with previously published data for ATRA-MPs manufactured by solvent evaporation (64-66). PLGA is widely used in research due to its biocompatibility and ability to encapsulate conventional drugs and proteins, as well as its mechanical strength allowing protection and controlled release of the cargo (67, 68). Following encapsulation of ATRA in PLGA MPs, the release profile was similar at both physiological and acidic pH indicating that ATRA would be released in the acidic environment of the phagosome and lysosome. Although the emitted dose of ATRA-MPs from a dry powder inhaler (DPI) was variable, the result of 53.7 ± 21.5 % compares favourably with a number of licenced DPIs where the total emitted dose was only 20 to 30% (69, 70). The addition of a lubricant such as magnesium stearate (71) or a desiccant (72) could provide more efficient de-agglomeration, enhanced flow and therefore more reproducible dosing.

Our *in vitro* testing indicated that ATRA solution (5 μg/ml ATRA) and ATRA MPs (containing the equivalent of 5 μg/ml ATRA) significantly reduced the growth of Mtb H37Ra in THP-1 macrophage cultures compared to untreated cells. The avirulent strain of Mtb was utilized *in vitro* as the group have previously demonstrated comparable anti-tubercular efficacy of PLGA MPs in THP-1 derived macrophages infected with both the avirulent (H37Ra) and virulent (H37Rv) strains (48) Whilst there are variations in the host response to each strain due to genetic differences, the results of the *in vitro* testing are are in keeping with those in the literature testing ATRA using a variety of strains such as Crowle at al. who found that ATRA solution (3 μg/ml) reduced the growth of Mtb Erdman in monocyte-derived macrophages (26). Wheelwright et al. also demonstrated an antimicrobial effect of ATRA in

both monocytes and monocyte-derived macrophages (MDMs) infected with Mtb H37Ra and Mtb H37Rv respectively, albeit at a lower concentration of ATRA (3 ng/ml) (28). In addition, a direct pathogen-targeted effect of ATRA was demonstrated by Greenstein et al. on the growth of Mtb complex strains in broth cultures, with a dose of 16 µg/ml proving most effective, reducing bacterial growth by 98% (33, 34).

Several studies have investigated the antimicrobial mechanism of action of ATRA in Mtb-infected macrophages *in vitro*. Wheelwright et al. found that ATRA reduced intracellular cholesterol levels, required as an energy source for Mtb (73), via the Niemann-Pick Disease Type 2C (NPC2) gene thus simultaneously depriving Mtb of an essential nutrient while boosting the ability of the macrophage to inhibit its growth via lysosomal acidification (28). In addition, we recently found that ATRA increases autophagy in Mtb-infected THP-1 cells in a Beclin1-dependent manner to inhibit Mtb growth (74). Estrella et al. combined ATRA with vitamin D3 treatment in THP-1 cells and found that reduced growth of H37Rv was associated with increased reactive oxygen species (ROS) production and autophagy and was associated with the formation of multi-nucleated giant cells (MNGCs). In the present study we found that ATRA alone, either in solution or encapsulated form, also stimulated MNGC formation with or without Mtb infection. MNGCs contribute to TB granuloma formation *in vivo* and, although their exact role in the process is unclear (75, 76), there is no doubting the importance of the granuloma in containing infection (77, 78). In a 2-dimensional (2-D) *in vitro* model it is difficult to fully define the impact of ATRA on granuloma formation. Whether this morphological change contributes to the host protective properties requires further investigation. In addition, secretion of the anti-inflammatory cytokine IL-10 was reduced *in vitro* following treatment of infected cells with ATRA solution, ATRA-MP and UNL-MP. Inhibition of IL-10 secretion allows phagolysosomal maturation to proceed as previously reported (79) and may contribute to the anti-microbial effect of ATRA . It seems likely, therefore, that ATRA could be exerting its antibacterial effects on Mtb in a variety of ways, utilising both host and pathogen-directed mechanisms.

Crucially, the anti-bacterial effects of both ATRA-MPs and ATRA solution were replicated *in vivo*; treatment significantly decreased the bacterial burden (CFU) of virulent Mtb (H37Rv) in the lungs of BALB/c mice following just three doses administered intratracheally. The effect was unaltered with the addition of the first-line antibiotic rifampicin, a promising result for ATRA as both a standalone and adjunctive treatment. While no significant difference was detected between treatment with ATRA in solution and ATRA-MPs 21 days post-infection, the anti-microbial benefits of encapsulated ATRA may accrue over a longer time span. Yamada et al. published one of the first known *in vivo* studies involving ATRA in Mtb infection using a rat model infected with the virulent H37Rv strain. The study demonstrated a significant decrease in bacterial burden in both the lung and spleen following repeated doses (alternate days) of orally administered ATRA (100 µg/100 g body weight) over a three- and five-week period (29). Knaul et al. also used ATRA, administered subcutaneously in the form of sustained release pellets, to deplete lung CD11b+Gr1+ myeloid derived suppressor cells (MDSCs) and saw increased numbers of T cells and local proliferation of lymphocytes as well as decreased bacterial burden and reduced pathology in susceptible 129S2 mice infected with H37Rv

(31). More recently, Mourik et al. assessed the benefits of adjunctive immunotherapy, including ATRA, in TB treatment using a BALB/c mouse model. ATRA pellets were administered subcutaneously (2 mg/kg) in combination with 1, 25(OH) 2-vitamin D_3 and α-galactosylceramide as immunotherapy plus isoniazid, rifampicin and pyrazinamide, compared to treatment with the antibiotics alone (30). At 5-weeks post-treatment the immunotherapy and antibiotic combination resulted in a trend towards a reduction in bacterial load in the lungs and by week 30 the relapse rate was 12.5 % compared to 75 % for conventional treatment alone (30). Each of these studies add to the growing body of evidence of the benefit of ATRA in TB treatment, however, to our knowledge this is the first work that explores the administration of ATRA via the airways in a TB infection model.

A fine balance of pro-inflammatory and anti-inflammatory responses are required concurrently within the host to control infection whilst avoiding excessive pathology. Histopathological examination of the lungs of BALB/C mice following treatment demonstrated that ATRA-MPs and ATRA plus rifampicin in solution administered intratracheally reduced the extent of pulmonary lesions. Yamada et al. reported less pathology following ATRA treatment in a rat model associated with an increased influx of T cells (CD4, CD8, α/β T, ɣ/δ T, CD25), Natural Killer cells and CD163 macrophages three weeks post-infection (29). One possible explanation for the amelioration of inflammation is the expansion of regulatory T cells (Tregs) by ATRA in the lungs (80). However, this does not explain the difference between ATRA solution alone and ATRA-MPs. Of potential significance here was the finding that both iNOS and TNF-α transcription were lower in the lung homogenates of ATRA-MP treated mice relative to mice treated with ATRA solution and a reduction in iNOS has been linked to improved pulmonary pathology in a model of acute lung injury (81). Our *in vitro* experiments and previously published data (48) indicate that, in addition to the effects of their encapsulated cargo, the PLGA MPs themselves influence immune cell function. Here, *in vitro*, IL-1β secretion was increased by UNL-MPs in infected macrophages, possibly reflecting a synergistic increase in TLR-mediated inflammasome activity, reported previously for PLGA MP and LPS signalling in DCs (82). While mature IL-1β is pro-inflammatory it also reduces bacterial burden in macrophage cultures which could improve immunopathology. Differences in post-translational modification of IL-1β would not have been reflected in IL-1β mRNA expression in the lungs.

Conclusions:

This study builds on existing data regarding the effect of ATRA as a TB treatment by bringing an advanced formulation of ATRA, in the form of an inhalable MP, from manufacture through to pre-clinical testing. The treatment here is administered via the pulmonary route *in vivo* offering an alternative to the traditional oral supplementation that has so far been ineffective in clinical studies. The results also show the benefit of ATRA as a practical treatment post-infection, and highlight the importance of appropriate nutrition in host-protective immune responses to TB disease. This is the first study to-date of a controlled release ATRA treatment for TB, suitable for inhalation that offers improved targeting of a HDT, retains antibacterial efficacy and reduces pulmonary pathology compared to ATRA solution.

Declarations of interest: None.

Acknowledgments: This work was supported by the Health Research Board in Ireland [grant numbers HRA_POR/2012/4]. AFM & SAC also acknowledge support from SFI [Grant codes 13/IA/1840 & 13/RC/20173].

Supplementary data

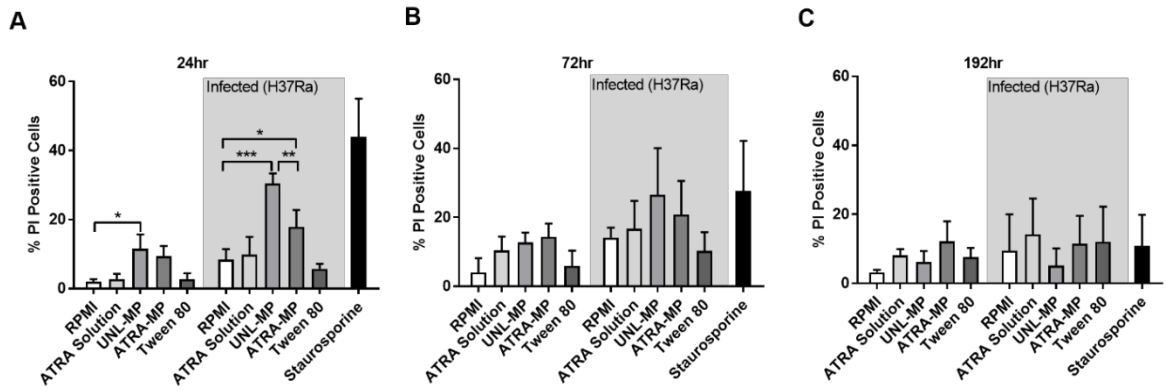


Figure S.1: The effect of ATRA treatment on macrophage viability *in vitro.* The proportion of dead cells (%) as determined by propidium iodide (dead cells) and Hoecsht (total cell counts) in the absence and presence of Mtb infection (H37Ra) at (A) 24 hrs, (B) 72 hrs and (C) 192 hrs post-treatment of THP-1 derived macrophages. Treatment included RPMI, ATRA solution (5 µg/ml), unloaded-MPs (UNL-MP) (=ATRA-MPs), ATRA-loaded MPs (ATRA-MP) (=5 µg/ml ATRA) and RPMI-Tween®80 (0.025 %). Staurosporine (0.4µg/ml) was utilized as a positive control in uninfected cells. The proportion of PI positive cells were calculated using the Cytell Cell Imaging System (GE Healthcare (n=3) with *$p < 0.05$, **$p < 0.01$ and ***$p < 0.001$.

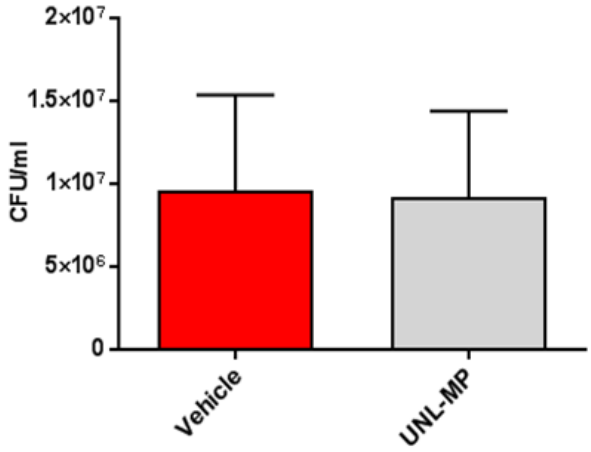


Figure S.2: Unloaded-MP (UNL-MP) efficacy studies. BALB/c mice infected with Mtb (H37Rv) were treated 14 days post-infection with vehicle only (NaCl 0.9 % + 0.05 % Tween®80) and UNL-MPs (218 mg/kg = 20 mg/kg of antitubercular cargo). Three doses of each treatment were administered 48 hrs apart. Bacterial viability was measured by harvesting Mtb from the lungs of the animals 21 days post-infection and plating on Middlebrook 7H11 agar, colonies were counted a further 21 days later, (n=5).

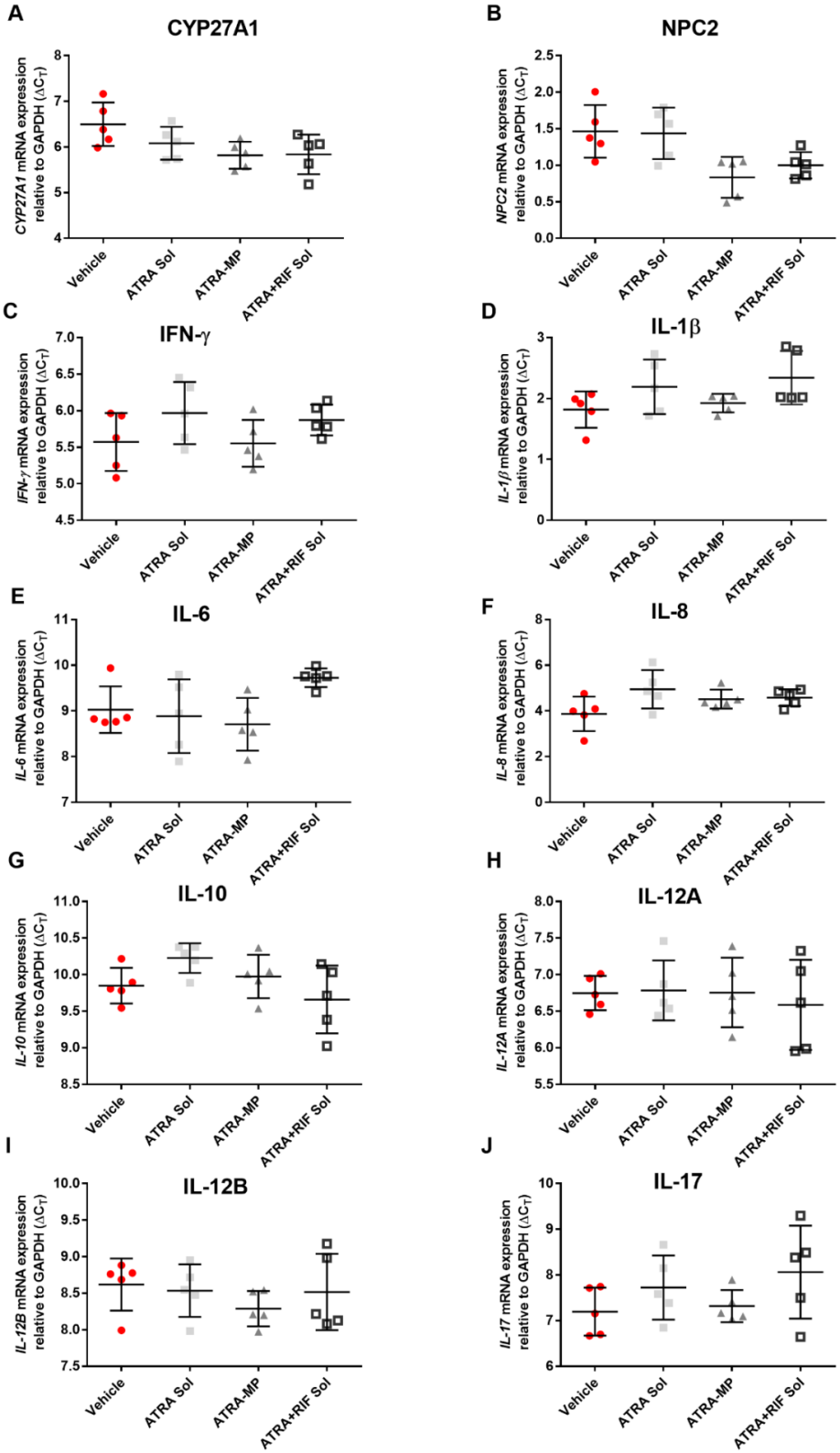


Figure S.3 *In vivo* mRNA transcription (non-significant) analysis following treatment of Mtb (H37Rv) infected BALB/C mice with vehicle (NaCl+Tween®80 0.05 %), ATRA solution (2.5 mg/kg), ATRA plus rifampicin solution (2.5 mg/kg + 12 mg/ml) and ATRA-loaded MPs (ATRA-MP) (=2.5 mg/kg ATRA). Real time PCR analysis was carried out on lung homogenates 21 days post-infection and expressed relative to GAPDH (Δ C_T). (A) iNOS, (B) TNF-α (n=5).

Table S.1: The bactericidal effects of rifampicin formulations against Mtb infection *in vitro*. Baseline infection levels were measured at 3 hrs post-infection of THP-1 derived macrophages with H37Ra which was followed by the addition of treatment, Bacterial growth (%) was determined 24 hrs and 72 hrs post infection via Time to Positivity (TTP) results that were measured using the BacT/Alert® 3D system. Treatment groups included RPMI, rifampicin solution (0.625 µg/ml) and rifampicin-MPs (RIF-MP) (=0.625 µg/ml rifampicin). (I) MOI:1-4/cell, (II) MOI: 1-5/cell and (III) MOI: 1-7/cell (n=3).

	Time to Positivity (Days)		
Treatment	**I**	**II**	**III**
3hrs			
RPMI	11.33	11.16	8.82
24hrs			
RPMI	10.66	17.99	10.32
RIF Solution	*Not detected*	*Not detected*	36.34
RIF-MP	*Not detected*	*Not detected*	24.66
72hrs			
RPMI	10.33	9.33	7.16
RIF Solution	*Not detected*	*Not detected*	*Not detected*
RIF-MP	*Not detected*	*Not detected*	32.5

References

1. UN. Sustainable Development Goals: 17 Goals to transform our world http://www.un.org/sustainabledevelopment/health/2017 [29.06.17].
2. WHO. Tuberculosis Factsheet http://www.who.int/mediacentre/factsheets/fs104/en/2017 [October 2017:[Available from: http://www.who.int/mediacentre/factsheets/fs104/en/.
3. Pai M, Behr MA, Dowdy D, Dheda K, Divangahi M, Boehme CC, et al. Tuberculosis. Nat Rev Dis Primers. 2016;2:16076.
4. Dooley KE, Chaisson RE. Tuberculosis and diabetes mellitus: convergence of two epidemics. Lancet Infect Dis. 2009;9(12):737-46.
5. O'Leary SM, Coleman MM, Chew WM, Morrow C, McLaughlin AM, Gleeson LE, et al. Cigarette smoking impairs human pulmonary immunity to Mycobacterium tuberculosis. Am J Respir Crit Care Med. 2014;190(12):1430-6.
6. Cegielski JP, McMurray DN. The relationship between malnutrition and tuberculosis: evidence from studies in humans and experimental animals. Int J Tuberc Lung Dis. 2004;8(3):286-98.
7. Lonnroth K, Williams BG, Cegielski P, Dye C. A consistent log-linear relationship between tuberculosis incidence and body mass index. Int J Epidemiol. 2010;39(1):149-55.
8. Hawn TR, Shah JA, Kalman D. New tricks for old dogs: countering antibiotic resistance in tuberculosis with host-directed therapeutics. Immunol Rev. 2015;264(1):344-62.
9. Wallis RS, Hafner R. Advancing host-directed therapy for tuberculosis. Nat Rev Immunol. 2015;15(4):255-63.
10. Kaufmann SH, Lange C, Rao M, Balaji KN, Lotze M, Schito M, et al. Progress in tuberculosis vaccine development and host-directed therapies--a state of the art review. Lancet Respir Med. 2014;2(4):301-20.
11. O'Connor G, Gleeson LE, Fagan-Murphy A, Cryan SA, O'Sullivan MP, Keane J. Sharpening nature's tools for efficient tuberculosis control: A review of the potential role and development of host-directed therapies and strategies for targeted respiratory delivery. Adv Drug Deliv Rev. 2016;102:33-54.
12. Singhal A, Jie L, Kumar P, Hong GS, Leow MK, Paleja B, et al. Metformin as adjunct antituberculosis therapy. Sci Transl Med. 2014;6(263):263ra159.
13. Vashisht R, Brahmachari SK. Metformin as a potential combination therapy with existing front-line antibiotics for Tuberculosis. J Transl Med. 2015;13:83.
14. Skerry C, Pinn ML, Bruiners N, Pine R, Gennaro ML, Karakousis PC. Simvastatin increases the in vivo activity of the first-line tuberculosis regimen. J Antimicrob Chemother. 2014;69(9):2453-7.
15. Dutta NK, Bruiners N, Pinn ML, Zimmerman MD, Prideaux B, Dartois V, et al. Statin adjunctive therapy shortens the duration of TB treatment in mice. J Antimicrob Chemother. 2016.
16. Vilaplana C, Marzo E, Tapia G, Diaz J, Garcia V, Cardona PJ. Ibuprofen therapy resulted in significantly decreased tissue bacillary loads and increased survival in a new murine experimental model of active tuberculosis. J Infect Dis. 2013;208(2):199-202.
17. Dutta NK, Kumar KA, Mazumdar K, Dastidar SG. In vitro and in vivo antimycobacterial activity of antiinflammatory drug, diclofenac sodium. Indian J Exp Biol. 2004;42(9):922-7.
18. Koh WJ, Kwon OJ, Suh GY, Chung MP, Kim H, Lee NY, et al. Six-month therapy with aerosolized interferon-gamma for refractory multidrug-resistant pulmonary tuberculosis. J Korean Med Sci. 2004;19(2):167-71.
19. Suarez-Mendez R, Garcia-Garcia I, Fernandez-Olivera N, Valdes-Quintana M, Milanes-Virelles MT, Carbonell D, et al. Adjuvant interferon gamma in patients with drug - resistant pulmonary tuberculosis: a pilot study. BMC Infect Dis. 2004;4:44.
20. Condos R, Rom WN, Schluger NW. Treatment of multidrug-resistant pulmonary tuberculosis with interferon-gamma via aerosol. Lancet. 1997;349(9064):1513-5.

21. Johnson BJ, Ress SR, Willcox P, Pati BP, Lorgat F, Stead P, et al. Clinical and immune responses of tuberculosis patients treated with low-dose IL-2 and multidrug therapy. Cytokines Mol Ther. 1995;1(3):185-96.
22. Johnson B, Bekker LG, Ress S, Kaplan G. Recombinant interleukin 2 adjunctive therapy in multidrug-resistant tuberculosis. Novartis Found Symp. 1998;217:99-106; discussion -11.
23. Aibana O, Franke MF, Huang CC, Galea JT, Calderon R, Zhang Z, et al. Impact of Vitamin A and Carotenoids on the Risk of Tuberculosis Progression. Clin Infect Dis. 2017.
24. Tretinoin [Internet]. The Pharmaceutical Press. 2017 [cited 01.07.17].
25. Semba RD. Vitamin A as "anti-infective" therapy, 1920-1940. J Nutr. 1999;129(4):783-91.
26. Crowle AJ, Ross EJ. Inhibition by retinoic acid of multiplication of virulent tubercle bacilli in cultured human macrophages. Infect Immun. 1989;57(3):840-4.
27. Estrella JL, Kan-Sutton C, Gong X, Rajagopalan M, Lewis DE, Hunter RL, et al. A Novel in vitro Human Macrophage Model to Study the Persistence of Mycobacterium tuberculosis Using Vitamin D(3) and Retinoic Acid Activated THP-1 Macrophages. Front Microbiol. 2011;2:67.
28. Wheelwright M, Kim EW, Inkeles MS, De Leon A, Pellegrini M, Krutzik SR, et al. All-trans retinoic acid-triggered antimicrobial activity against Mycobacterium tuberculosis is dependent on NPC2. J Immunol. 2014;192(5):2280-90.
29. Yamada H, Mizuno S, Ross AC, Sugawara I. Retinoic acid therapy attenuates the severity of tuberculosis while altering lymphocyte and macrophage numbers and cytokine expression in rats infected with Mycobacterium tuberculosis. J Nutr. 2007;137(12):2696-700.
30. Mourik BC, Leenen PJ, De Knegt GJ, Huizinga R, Van der Eerden BC, Wangk J, et al. Immunotherapy Added to Antibiotic Treatment Reduces Relapse of Disease in a Mouse Model of Tuberculosis. Am J Respir Cell Mol Biol. 2016;56(2):233-41.
31. Knaul JK, Jorg S, Oberbeck-Mueller D, Heinemann E, Scheuermann L, Brinkmann V, et al. Lung-residing myeloid-derived suppressors display dual functionality in murine pulmonary tuberculosis. Am J Respir Crit Care Med. 2014;190(9):1053-66.
32. Anand PK, Kaul D. Downregulation of TACO gene transcription restricts mycobacterial entry/survival within human macrophages. FEMS Microbiol Lett. 2005;250(1):137-44.
33. Greenstein RJ, Su L, Brown ST. Vitamins A & D inhibit the growth of mycobacteria in radiometric culture. PLoS One. 2012;7(1):e29631.
34. Greenstein RJ, Su L, Shahidi A, Brown WD, Clifford A, Brown ST. Unanticipated Mycobacterium tuberculosis complex culture inhibition by immune modulators, immune suppressants, a growth enhancer, and vitamins A and D: clinical implications. Int J Infect Dis. 2014;26:37-43.
35. Suarez S, O'Hara P, Kazantseva M, Newcomer CE, Hopfer R, McMurray DN, et al. Airways delivery of rifampicin microparticles for the treatment of tuberculosis. J Antimicrob Chemother. 2001;48(3):431-4.
36. Muttil P, Kaur J, Kumar K, Yadav AB, Sharma R, Misra A. Inhalable microparticles containing large payload of anti-tuberculosis drugs. Eur J Pharm Sci. 2007;32(2):140-50.
37. Lawlor C, O'Sullivan MP, Rice B, Dillon P, Gallagher PJ, O'Leary S, et al. Therapeutic aerosol bioengineering of targeted, inhalable microparticle formulations to treat Mycobacterium tuberculosis (MTb). J Mater Sci Mater Med. 2012;23(1):89-98.
38. Hickey AJ, Durham PG, Dharmadhikari A, Nardell EA. Inhaled drug treatment for tuberculosis: Past progress and future prospects. J Control Release. 2015.
39. Edwards DA, Dunbar C. Bioengineering of therapeutic aerosols. Annual review of biomedical engineering. 2002;4:93-107.
40. O'Hara P, Hickey AJ. Respirable PLGA microspheres containing rifampicin for the treatment of tuberculosis: manufacture and characterization. Pharm Res. 2000;17(8):955-61.
41. Sharma R, Yadav AB, Muttil P, Kajal H, Misra A. Inhalable microparticles modify cytokine secretion by lung macrophages of infected mice. Tuberculosis (Edinb). 2011;91(1):107-10.

42. Ricci M, Giovagnoli S, Blasi P, Schoubben A, Perioli L, Rossi C. Development of liposomal capreomycin sulfate formulations: effects of formulation variables on peptide encapsulation. Int J Pharm. 2006;311(1-2):172-81.
43. Gaspar DP, Faria V, Goncalves LM, Taboada P, Remunan-Lopez C, Almeida AJ. Rifabutin-loaded solid lipid nanoparticles for inhaled antitubercular therapy: Physicochemical and in vitro studies. Int J Pharm. 2016;497(1-2):199-209.
44. Dharmadhikari AS, Kabadi M, Gerety B, Hickey AJ, Fourie PB, Nardell E. Phase I, single-dose, dose-escalating study of inhaled dry powder capreomycin: a new approach to therapy of drug-resistant tuberculosis. Antimicrob Agents Chemother. 2013;57(6):2613-9.
45. Erkelens MN, Mebius RE. Retinoic Acid and Immune Homeostasis: A Balancing Act. Trends Immunol. 2017;38(3):168-80.
46. Visser ME, Grewal HM, Swart EC, Dhansay MA, Walzl G, Swanevelder S, et al. The effect of vitamin A and zinc supplementation on treatment outcomes in pulmonary tuberculosis: a randomized controlled trial. Am J Clin Nutr. 2011;93(1):93-100.
47. Lawson L, Thacher TD, Yassin MA, Onuoha NA, Usman A, Emenyonu NE, et al. Randomized controlled trial of zinc and vitamin A as co-adjuvants for the treatment of pulmonary tuberculosis. Trop Med Int Health. 2010;15(12):1481-90.
48. Lawlor C, O'Connor G, O'Leary S, Gallagher PJ, Cryan SA, Keane J, et al. Treatment of Mycobacterium tuberculosis-Infected Macrophages with Poly(Lactic-Co-Glycolic Acid) Microparticles Drives NFkappaB and Autophagy Dependent Bacillary Killing. PLoS One. 2016;11(2):e0149167.
49. Khan A, Sarkar S, Sarkar D. Bactericidal activity of 2-nitroimidazole against the active replicating stage of Mycobacterium bovis BCG and Mycobacterium tuberculosis with intracellular efficacy in THP-1 macrophages. Int J Antimicrob Agents. 2008;32(1):40-5.
50. Ryan RC, O'Sullivan MP, Keane J. Mycobacterium tuberculosis infection induces non-apoptotic cell death of human dendritic cells. BMC Microbiol. 2011;11:237.
51. Parthasarathy R, Gilbert B, Mehta K. Aerosol delivery of liposomal all-trans-retinoic acid to the lungs. Cancer Chemother Pharmacol. 1999;43(4):277-83.
52. March TH, Cossey PY, Esparza DC, Dix KJ, McDonald JD, Bowen LE. Inhalation administration of all-trans-retinoic acid for treatment of elastase-induced pulmonary emphysema in Fischer 344 rats. Exp Lung Res. 2004;30(5):383-404.
53. Raleigh SM, Verschoyle RD, Bowskill C, Pastorino U, Staniforth JN, Steele F, et al. Pulmonary availability of isotretinoin in rats after inhalation of a powder aerosol. Br J Cancer. 2000;83(7):935-40.
54. Massaro GD, Massaro D. Retinoic acid treatment abrogates elastase-induced pulmonary emphysema in rats. Nat Med. 1997;3(6):675-7.
55. Schaffer MW, Roy SS, Mukherjee S, Ong DE, Das SK. Uptake of all-trans retinoic acid-containing aerosol by inhalation to lungs in a guinea pig model system--a pilot study. Exp Lung Res. 2010;36(10):593-601.
56. Frankenberger M, Heimbeck I, Moller W, Mamidi S, Kassner G, Pukelsheim K, et al. Inhaled all-trans retinoic acid in an individual with severe emphysema. Eur Respir J. 2009;34(6):1487-9.
57. Seegmiller RE, Ford WH, Carter MW, Mitala JJ, Powers WJ, Jr. A developmental toxicity study of tretinoin administered topically and orally to pregnant Wistar rats. J Am Acad Dermatol. 1997;36(3 Pt 2):S60-6.
58. Lawlor C, O'Sullivan MP, Sivadas N, O'Leary S, Gallagher PJ, Keane J, et al. The application of high-content analysis in the study of targeted particulate delivery systems for intracellular drug delivery to alveolar macrophages. Mol Pharm. 2011;8(4):1100-12.
59. Russell DG, Vanderven BC, Glennie S, Mwandumba H, Heyderman RS. The macrophage marches on its phagosome: dynamic assays of phagosome function. Nat Rev Immunol. 2009;9(8):594-600.

60. Ohashi K, Kabasawa T, Ozeki T, Okada H. One-step preparation of rifampicin/poly(lactic-co-glycolic acid) nanoparticle-containing mannitol microspheres using a four-fluid nozzle spray drier for inhalation therapy of tuberculosis. J Control Release. 2009;135(1):19-24.
61. Verma RK, Kaur J, Kumar K, Yadav AB, Misra A. Intracellular time course, pharmacokinetics, and biodistribution of isoniazid and rifabutin following pulmonary delivery of inhalable microparticles to mice. Antimicrob Agents Chemother. 2008;52(9):3195-201.
62. Garcia Contreras L, Sung J, Ibrahim M, Elbert K, Edwards D, Hickey A. Pharmacokinetics of Inhaled Rifampicin Porous Particles for Tuberculosis Treatment: Insight into Rifampicin Absorption from the Lungs of Guinea Pigs. Mol Pharm. 2015;12(8):2642-50.
63. Parumasivam T, Leung SS, Quan DH, Triccas JA, Britton WJ, Chan HK. Rifapentine-loaded PLGA microparticles for tuberculosis inhaled therapy: Preparation and in vitro aerosol characterization. Eur J Pharm Sci. 2016;88:1-11.
64. Cirpanli Y, Unlu N, Calis S, Hincal AA. Formulation and in-vitro characterization of retinoic acid loaded poly (lactic-co-glycolic acid) microspheres. J Microencapsul. 2005;22(8):877-89.
65. Jeong YI, Song JG, Kang SS, Ryu HH, Lee YH, Choi C, et al. Preparation of poly(DL-lactide-co-glycolide) microspheres encapsulating all-trans retinoic acid. Int J Pharm. 2003;259(1-2):79-91.
66. Daskin D, Gunduz U. Preparation and evaluation of polymer based microcarriers for all-trans-retinoic acid. Pharm Dev Technol. 2013;18(5):1017-25.
67. Makadia H, Siegel S. Poly Lactic-co-Glycolic Acid (PLGA) as Biodegradable Controlled Drug Delivery Carrier. Polymers. 2011;3:1377-97.
68. Puppi D, Piras AM, Detta N, Dinucci D, Chiellini F. Poly(lactic-co-glycolic acid) electrospun fibrous meshes for the controlled release of retinoic acid. Acta Biomater. 2010;6(4):1258-68.
69. Hassoun M, Ho S, Muddle J, Buttini F, Parry M, Hammond M, et al. Formulating powder-device combinations for salmeterol xinafoate dry powder inhalers. Int J Pharm. 2015;490(1-2):360-7.
70. Abdelrahim ME. Emitted dose and lung deposition of inhaled terbutaline from Turbuhaler at different conditions. Respir Med. 2010;104(5):682-9.
71. Buttini F, Brambilla G, Copelli D, Sisti V, Balducci AG, Bettini R, et al. Effect of Flow Rate on In Vitro Aerodynamic Performance of NEXThaler((R)) in Comparison with Diskus((R)) and Turbohaler((R)) Dry Powder Inhalers. J Aerosol Med Pulm Drug Deliv. 2016;29(2):167-78.
72. Nolan LM, Li J, Tajber L, Corrigan OI, Healy AM. Particle engineering of materials for oral inhalation by dry powder inhalers. II-Sodium cromoglicate. Int J Pharm. 2011;405(1-2):36-46.
73. Pandey AK, Sassetti CM. Mycobacterial persistence requires the utilization of host cholesterol. Proc Natl Acad Sci U S A. 2008;105(11):4376-80.
74. Coleman MM, Basdeo SA, Coleman AM, Ní Cheallaigh C, Peral de Castro C, McLaughlin AM, Dunne PJ, Harris J, Keane J. All-trans Retinoic Acid Augments Autophagy during Intracellular Bacterial Infection. Am J Respir Cell Mol Biol. 2018 May 31.PMID 29852080.
75. Kumarguru BN, Natarajan M, Biligi DS, Raghupathi AR. Giant Cell Lesions of Lungs: A Histopathological and Morphometric Study of Seven Autopsy Cases. J Clin Diagn Res. 2015;9(11):EC12-6.
76. Miranda MS, Breiman A, Allain S, Deknuydt F, Altare F. The Tuberculous Granuloma: An Unsuccessful Host Defence Mechanism Providing a Safety Shelter for the Bacteria? Journal of Immunology Research. 2012;2012.
77. Ulrichs T, Kaufmann SH. New insights into the function of granulomas in human tuberculosis. J Pathol. 2006;208(2):261-9.
78. Tsai MC, Chakravarty S, Zhu G, Xu J, Tanaka K, Koch C, et al. Characterization of the tuberculous granuloma in murine and human lungs: cellular composition and relative tissue oxygen tension. Cell Microbiol. 2006;8(2):218-32.
79. O'Leary S, O'Sullivan MP, Keane J. IL-10 blocks phagosome maturation in mycobacterium tuberculosis-infected human macrophages. Am J Respir Cell Mol Biol. 2011;45(1):172-80.

80. Coleman MM, Ruane D, Moran B, Dunne PJ, Keane J, Mills KH. Alveolar macrophages contribute to respiratory tolerance by inducing FoxP3 expression in naive T cells. Am J Respir Cell Mol Biol. 2013;48(6):773-80.
81. Zhang HX, Liu SJ, Tang XL, Duan GL, Ni X, Zhu XY, et al. H2S Attenuates LPS-Induced Acute Lung Injury by Reducing Oxidative/Nitrative Stress and Inflammation. Cellular physiology and biochemistry : international journal of experimental cellular physiology, biochemistry, and pharmacology. 2016;40(6):1603-12.
82. Sharp FA, Ruane D, Claass B, Creagh E, Harris J, Malyala P, et al. Uptake of particulate vaccine adjuvants by dendritic cells activates the NALP3 inflammasome. Proc Natl Acad Sci U S A. 2009;106(3):870-5.